The Feasibility of an Arctic Based Wind-Powered Pump to Thicken the Ice Sheet in an Effort to Reduce the Impact of Global Warming

Ellis Cole, Euan Cuthbertson, Alexander Daniels and Edward Wright

Internal Supervisor: Dr Iestyn Pierce

External Supervisor: Nick Penny

School of Electronic Engineering

Bangor University

2017

Acknowledgements

We would like to give a huge thanks to our external project supervisor Nick Penny for his continuous support and commitment put towards the whole project. Without his help and uncanny enthusiasm, much of the project would not have been possible. Also, thanks to Tim Jepson for some invaluable guidance for the experimental aspects of the project, and Ankita Goyal, for her assistance with the business side of the project.

Statement of Originality

The work presented in this report is entirely from the studies of the individual student, except where otherwise stated. Where derivations are presented, and the origin of the work is either wholly or in part from other sources, then full reference is given to the original author. This work has not been presented previously for any degree, nor is it at present under consideration by any other degree awarding body.

Signed:

Statement of Availability

I hereby acknowledge the availability of any part of this report for viewing, photocopying or incorporation into future studies, providing that full reference is given to the origins of any information contained herein.

Signed:

Abstract

This project aims to evaluate the feasibility of an Arctic based wind-powered pump in an effort to thicken the ever-shrinking Artic ice sheets to reduce the impact of Global Warming. This technology's main application is to prevent further loss of ice which would lead to less solar radiation being reflected back into space. Current research suggests attempts at thickening the Arctic sea ice would not be feasible due to astronomical costs.

To explore the possibility of using a wind-powered pump, the project analyses Arctic wind data, to see if there is enough potential wind power in the Arctic. Different wind turbines were also looked at, in an attempt to find the most efficient way to obtain this power. Also, many distribution systems were analysed, to see the best way to spread the pumped seawater over the Arctic's surface. Preventions from harsh Arctic conditions affecting the system were mentioned, as well as ways of measuring ice thickness. These ideas were brought together to try and demonstrate a 1/8th scale model.

The main research results completed are in this report, as well as any experimental findings. Furthermore, a final 1/8th scale design is shown with details on size dimensions and the potential of it on the full scale. Any instrumentation put on the device is documented with designs shown for future use. A short business model looking at the costs of the project and how the systems will be maintained and worked on is also included.

Table of Contents

The Feasibility of an Arctic Based Wind-Powered Pump to Thicken the Ice Sheet in an Effort to Reduce the Impact of Global Warming i
Acknowledgements ii
Statement of Originality iii
Statement of Availability iii
Abstract iv
Table of Contents v
Chapter 1: Introduction 1
1.1 Motivation and Rationale 1
1.2 Aim and Objectives 1
1.3 Report Outline 2
Chapter 2: Background Information 3
2.1 Albedo Effect 3
2.2 Global Warming 4
2.3 Power Generation 6
2.3.1 Wind Power 6
2.3.2 Solar 7
2.3.3 Seebeck generator 8
2.3.4 Water Turbine 9
2.4 Arctic Sea Water 10
2.4.1 Freezing 10
2.4.2 Thawing 11
2.4.3 Electrical Properties 12
2.4.4 Air Resistance 13
2.4.5 Laminar Flow 14
2.5 Mechanical Actuators 15
2.5.1 Pumps 15
2.5.2 Motors 18
2.6 Inuit Population 19

2.7 Literature Review 20
Chapter 3: Research and Further Reading 22
3.1 Arctic Weather 22
3.1.1 Wind 22
3.1.2 Temperature 24
3.2 Energy Requirements 24
3.3 Power Generation 25
3.3.1 Wind Generation Systems 25
3.3.1.1 Horizontal Axis Wind Turbines 25
3.3.1.2 Vertical Axis Wind Turbines 25
3.3.1.3 Pole 26
3.3.1.4 Kite 27
3.3.2 Peltier 28
3.3.3 Water Turbine 29
3.4 Water Manipulation 30
3.4.1 Water Extraction 30
3.4.1.1 Pump 30
3.4.2 Water Distribution 31
3.4.2.1 Sprinklers 31
3.4.2.2 Helicopter 32
3.5 Instrumentation 33
3.5.1 Inputs 33
3.5.1.1 Wind Speed 33
3.5.1.2 Ice Thickness 35
3.5.1.3 Temperature 40
3.5.1.4 Flow 41
3.5.1.5 Voltage 41

3.5.1.6 Current 43
3.5.2 Process 47
3.5.2.1 ADC 47
3.5.2.2 Raspberry Pi 48
3.5.2.3 SPI/I2C 50
3.5.3 Outputs 50
3.5.3.1 Motor Control 50
3.5.4 Communications 51
3.5.4.1 Mobile Ad-Hoc 51
3.5.4.2 Data (MQTT) 53
3.6 Business Information 53
Chapter 4: Design and Methodology 57
4.1 Design 57
4.1.1 Design 1 57
4.1.2 Design 2 58
4.1.3 Final Design 60
4.1.4 Instrumentation 61
4.1.4.1 Ice Thickness 61
4.1.4.2 Power 67
4.1.4.3 Temperature 70
4.2 Methodology 72
4.2.1 Instrumentation and Calibration 72
Results and Discussion 76
5.1 Lake Experiments 76
5.1.1 Experiment 1 76
5.1.1.1 Water Range 76
5.1.1.2 Water Flow Rate 77
5.1.1.3 Tube Length 79

5.1.2 Experiment 2 80

5.2 Discussion 80

Conclusion and Future Work 82

6.1 Conclusion 82

6.2 Future Work 82

References 84

Chapter 1: Introduction

1.1 Motivation and Rationale

Global Warming and Climate change are becoming an increasingly pressing issue in modern day society. In the past 50 years since the industrial revolution, the average global temperature has increased at the fastest rate that humans have recorded. To put this in context, all but one of the NASA's 16 hottest years that they have recorded in their 134 years of taking global measurements, have occurred after the turning of the millennium. [1]

This warming of the planet has had a drastic effect on our polar regions, with the Arctic ice extent decreasing by 1 million square kilometres since the year 2000. [2] This will have a knock-on effect on the sea levels over the planet, increasing them so that lowland areas around the world could become flooded. In addition, the loss of the Artic would have an enormous environmental impact on any animals that will lose their natural habitat, having a detrimental impact on the whole ecosystem.

It is for this reason that the research in this project has been undertaken to look at ways that the decrease of the Arctic sea ice could be slowed, or even stopped completely so that it could start to be rebuilt.

1.2 Aim and Objectives

The aim of the research project is to investigate the feasibility of a wind driven pump system that draws water up from underneath the ice sheets in the Arctic and distributes it on top of the ice, thickening the sheets and therefore decreasing the effect of global warming. The project explores different ways of distributing the water and any instrumentation that might be placed on the devices to measure their effectiveness. To achieve this aim, the following objectives are to be strived towards:

1) The production of a 1/8th scale model that distributes water in a 4m radius around the model, keeping within the power budget that is available.
2) The testing of such a model to ensure it reaches the specified distance and to investigate how much water it distributes.
3) To enable further research into a similar design by documenting instrumentation and providing a design framework that can be easily built upon and scaled up.

1.3 Report Outline

This report was laid out in the following manner: -

Chapter 1 – gives an introduction to the project, including reasons why it was undertaken as well as the aims and objectives of the project.

Chapter 2 – contains the background information on the project, including all associated theory and a literature review of related work.

Chapter 3 – contains all the research/reading that was done including the different approaches taken to the project and wind data from the Arctic, and information on the instrumentation present in the design.

Chapter 4 – includes all the designs of the project and the methodology of any experimentation that was completed.

Chapter 5 – includes the results of the experiments along with discussions of any findings.

Chapter 6 – comprises of a summary of the project, the challenges and the limitations that were faced, the conclusions that were drawn and the future work that could be done.

Chapter 2: Background Information

2.1 Albedo Effect

The albedo effect is a measure of the reflectivity of a surface, with different materials having a unique albedo. This albedo is unitless and varies between 0 and 1 and is commonly referred to as the 'whiteness' of a material, 0 being a black and highly absorbing material while 1 is a white and totally reflecting material [3].

Surfaces such as open Ocean have a much smaller albedo when compared to snow or sea ice. This means that much less solar radiation will reflect off the surface with the smaller albedo. This additional absorption of solar radiation results in increasing temperatures, which is known as the sea-ice albedo feedback. This is a feedback climate process which may serve to amplify the retreat of sea-ice in the Arctic. [4]

The open ocean has an albedo of 0.06, meaning that it reflects approximately 6% of solar radiation it succumbs. Sea ice reflects more incident sunlight than water, and its albedo is up to 0.5. Snow is also different, due to its white colour sunlight will reflect a lot more on this surface than the darker ocean and sea ice. Fresh snow has an albedo of 0.9 meaning it will reflect up to 90% of incident sunlight. If there is less ice, the positive ice-albedo effect might amplify the decrease in ice coverage [5].

Snow is often present on top of sea-ice, and this slows down the rate at which the sea-ice melts. This is because when the snow melts, melt ponds are produced. Once these start to form, the albedo drops to around 0.75 which is still above the albedo of bare sea-ice [5]. As more snow and ice melts, the melt ponds will grow deeper, decreasing the albedo further and increasing the rate of melting. The difference a snow coverage on sea-ice makes to the albedo is shown in Figure 2.1 below when compared to bare-ice [6].

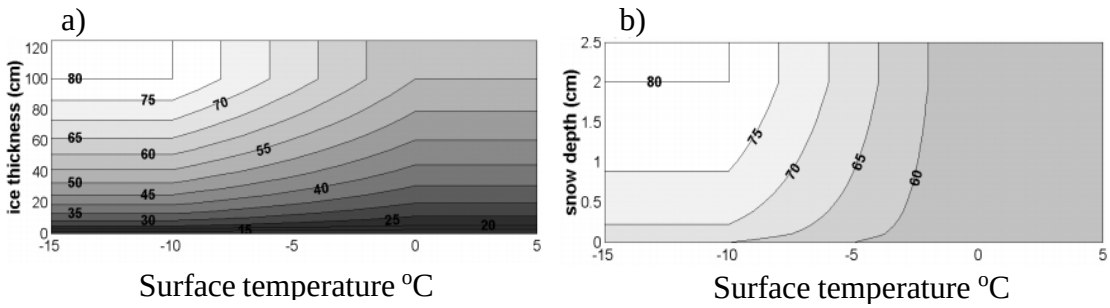

Figure 2.1 Variation of surface albedo (%) with a) ice thickness and surface temperature for a high-latitude Ocean, b) snow depth and surface temperature for lands covered by ice sheets. [3]

2.2 Global Warming

Global warming is a phenomenon that affects the entire world. It is described by the Oxford dictionary as “A gradual increase in the overall temperature of the Earth's atmosphere generally attributed to the greenhouse effect caused by increased levels of carbon dioxide, CFCs, and other pollutants.” [7] The Earth goes through periods of warming and freezing in its natural cycle as shown in Figure 2.2.

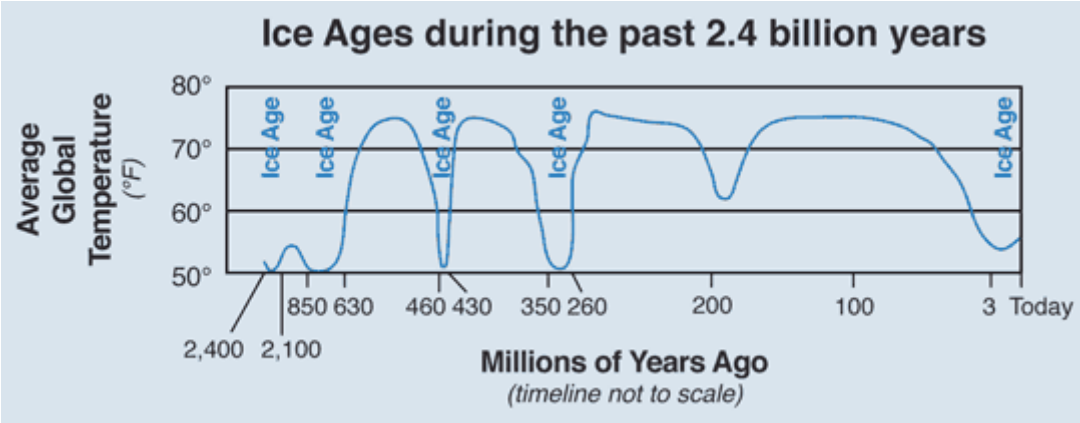

Figure 2.2 A chart to show the number of ice ages over the last 2.4 billion years [8]

There are a few factors that contribute to the temperature of the Earth. The first being changes in its orbit around the Sun, which effect where solar radiation hits the planet. This alone wouldn’t have a large affect, but coupled with the melting of snow due to the initial increase in temperature, and so the decrease in the overall albedo of the Earth, a reduction in the reflected solar radiation would occur, further heating the Earth.

The second and most important factor that contributes to global warming is the composition of the atmosphere. At the current time, the atmosphere is composed of 78.1% nitrogen and 20.9% oxygen. This leaves 1% left, and in this there is 9000ppm argon, accounting for most of what remains. The last 0.1% is the most important when it comes to the effects of climate change as it contains several greenhouse gases, with carbon dioxide (C02) taking up the largest part of it at 380ppm. These greenhouse gases are partially opaque to heat radiation, which means that part of the heat that tries to leave the Earth is radiated back towards it, therefore heating it up. This process is critical to the Earth, without it the surface would be covered in ice. However, the sharp increase in CO2 that has happened since the industrial revolution, an increase in the region of 100ppm, has contributed significantly to the recent temperature rise. Figure 2.3 shows this.

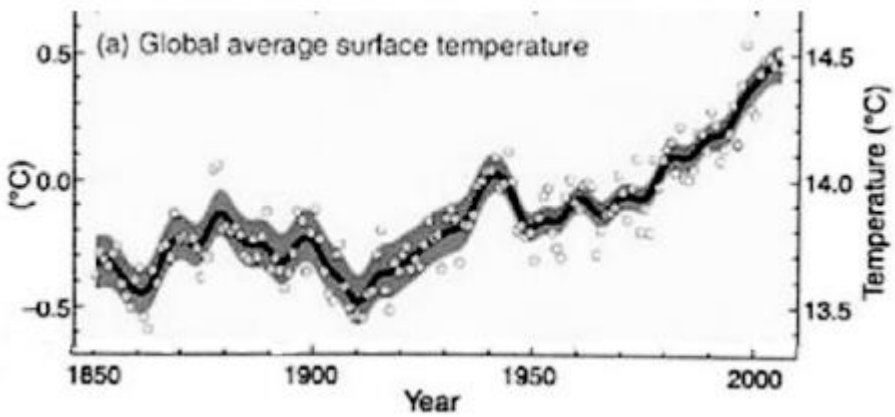

Figure 2.3 Changes in global temperature since 1850 [9]

This increase in temperature has led to a drastic fall off in the amount of sea ice that we see in the Arctic. The National Snow and Ice Data Centre (NSIDC) has conducted much research into the Arctic. It is a body that supports and carries out research into every bit of the Earth that is considered frozen, from snow and ice to glaciers and the climate processes that make up the cryosphere. Since 1979 it has tracked the sea ice extent daily, and from their data, Figure 2.4 was produced. The graph quite clearly shows a huge reduction in the extent of the ice. From the graph, it seems that at least 1million square kilometres of ice have been lost since the year 2000, which is an enormous amount. This is due to the effects that the rise in temperature shown in Figure 2.3 has produced. Although there has been no significant increase in temperature since 2003, the lower amounts of ice mean that a downwards trend is produced due to the lower albedo that the water has which effects the ice more and more the less of it there is.

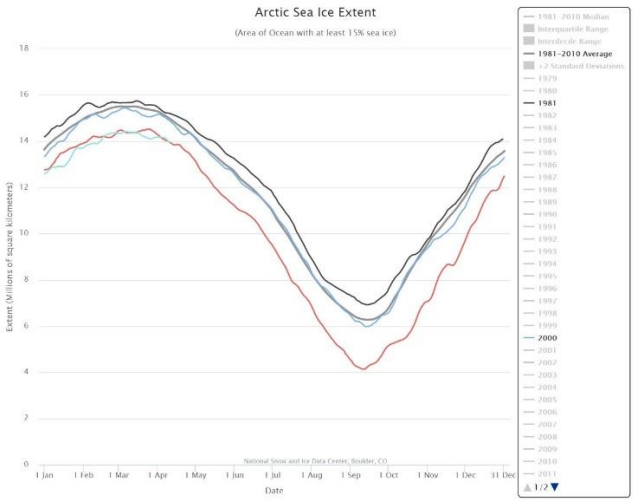

Figure 2.4 A graph showing the Arctic Sea Ice Extent in different years, the key does not show the red line as 2016, and the light blue one as 2017 so far. [2]

2.3 Power Generation

2.3.1 Wind Power

The Wind has been used for the last 1000 years as a source of energy with windmills taking advantage of the consistent renewable energy source. Since the end of the last century, the number of wind turbines is steadily on the rise and is becoming an important energy source for power generation in many countries. The amount of power available from the wind depends on three key factors, the volume of air, the speed of air and the density of air. The kinetic energy of a mass with a given velocity is

$$E_k = \frac{1}{2}mv^2$$

The mass of the wind that flows through the turbine per unit time is given by:

$$\frac{dm}{dt} = pAv$$

Where p is the density of the air, A is the rotor swept area of the turbine and v the velocity of the wind. From this the wind power can be calculated as power is the kinetic energy per unit time.

$$\mathrm{P} = \frac{1}{2}\, pAv^3$$

Any wind turbine does not generate power at 100% efficiency, and therefore this only gives the power available to the turbine. The power coefficient, C_p, is the ratio of power extracted by the turbine to the power available and this determines how efficient the wind turbine is. This value is limited to 59%, and this is known as the Betz Limit with no wind turbine able to exceed this value. [10]

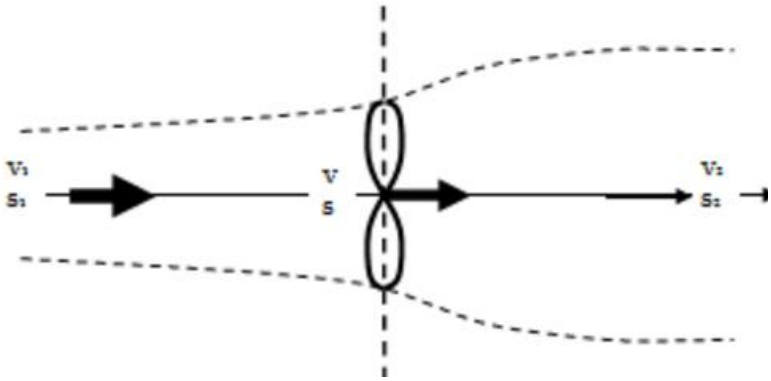

Figure 2.5 A diagram of wind turbine of area A and the wind before and after passing through the turbine, from [11]

The speed of wind slows down after passing through the turbine of area A, from velocity V_1 to V_2. Due to the mass flow being continuous as the velocity decreases, the area of air must increase. The difference between the two wind powers is known as the effective power and is given by:

$$\mathrm{P}eff = P_1 - P_2 = \frac{\Delta Vp}{2\Delta t}(v_1^2 - v_2^2) = \frac{pA}{4}(v_1 + v_2)(v_1^2 - v_2^2)$$

If there is no difference in the speeds of air before and after the turbine, then there is no change in net efficiency. If the difference is too big, then the flow of air is hindered too much. The relative drawing power is characterised by the power coefficient C_p.

$$C_p = \frac{P_{eff}}{P_{ava}} = \frac{(v_1 + v_2)(v_1^2 - v_2^2)}{2v_1^3} = \frac{(1 + x)(1 - x^2)}{2}$$

The maximum point of the equation above needs to be calculated so the maximum efficiency can be solved. The derivative is taken which gives a maximum when x is a value of 0.3. Maximum drawing power is achieved when $v_2 = v_1 / 3$. [10]

$$C_P = \frac{16}{27} = 59\%$$

2.3.2 Solar

Solar generates power by converting energy from sunlight into electricity, most commonly by using Photovoltaics which take advantage of the photovoltaic effect. Incident sunlight shines on the solar panels consisting of photons with energy,

$$E = hf$$

where h is the Planck constant (6.63×10^{-34} m^2 kgs^{-1}) and f is the frequency (Hz) of the light. These photons are absorbed by electrons in the solar panel, which in turn excites the electron to a higher state. An electric potential is then produced due to a separation of charges.

This possible source of renewable energy was looked at before being quickly discounted. This is due to the plan of the project pumping water in the winter months, where there is no sunlight. Therefore, solar cannot be used as the source of energy.

2.3.3 Seebeck generator

Another possible form of generating electricity in the Arctic is by using the differences in temperature that can be observed there and converting them into electricity. This is done using a Seebeck generator, which utilises the Seebeck effect, a type of thermoelectric effect. These devices require three main parts to ensure their operation. These are thermoelectric materials, thermoelectric modules and systems that can interface with the heat source.

Thermoelectric materials produce electricity while they are in a temperature gradient, in simpler terms they will only produce electricity if there is a temperature difference inside them. To be good at doing this, such materials must have a very rare combination of being both a high electrical conductor but a low thermal conductor. In a thermoelectric device, electrons flow from hot to cold, and the extent to which they do is governed by the Seebeck coefficient (S). This is defined as the voltage built up when a temperature gradient is applied to a material, and when the material has come to a steady state. The equation is shown below where ΔV is the voltage gradient present in the material, and ΔT is the temperature gradient.

$$S = -\frac{\Delta V}{\Delta T}$$

These thermoelectric materials are contained in a thermoelectric module that uses the characteristics of the material to output usable electricity. These modules are subjected to very large temperature gradients and due to this also experience very large stresses and strains, sometimes for extended periods of time. They must also be able to withstand these thermal cycles a great many times, increasing the chance the device may encounter mechanical failure. In order to function, a thermoelectric module requires two of these materials, an n-type and a p-type semiconductor. This ensures that a continuous circuit can be created in which current flows through the entire circuit. If only one type was used then a voltage would be induced but no current would be able to flow. The two semiconductors form a thermoelectric “couple” but don’t form a p-n junction. Inside the module, the two thermoelectric materials must be electrically in series but thermally in parallel, using internal wiring to accomplish this.

Using these systems, a Seebeck generator takes in heat from a source, in an Arctic environment it would be the warmer sea compared to the ice, and output electricity using

thermoelectric modules. To achieve maximum efficiency in the design heat exchangers are normally used on both the hot and the cold side. [12]

2.3.4 Water Turbine

One potential method of harvesting energy from the environment is a water turbine. Similar in construction to wind turbines, water turbines convert the kinetic energy of moving water into electrical energy by using turbine blades which rotate a motor generating electricity for use. Usually found in hydroelectricity plants, water turbines rely on the potential energy of the water in a raised reservoir. The water falls down pipes turning the potential energy into kinetic energy which then turns the turbine.

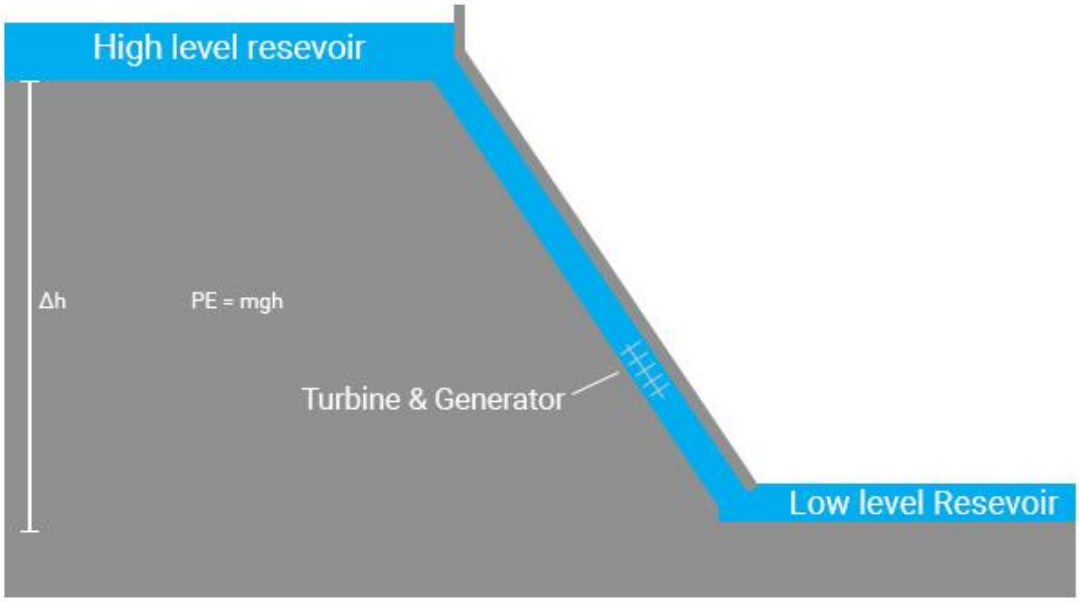

Figure 2.6 Hydroelectric Power Station Diagram

Figure 2.6 shows a diagram of a hydroelectric power station. The high-level reservoir has water with potential energy.

$$PE = mg\Delta h$$

All the potential energy is converted into kinetic energy as the water falls down the pipe making the potential energy and the kinetic energy equal.

$$PE = KE$$

The kinetic energy is what turns the turbine.

$$KE = \frac{1}{2}mv^2$$

2.4 Arctic Sea Water

2.4.1 Freezing

The freezing temperature of Arctic seawater is -1.8 degrees Celsius (28.7 degrees Fahrenheit) due to the salinity being approximately 30-34ppt. The amount and rate at which ice is formed depends on the way heat is exchanged, and the rate at which it grows can be estimated from thermodynamic growth, expressing the vertical growth of sea-ice using the formula:

$$\mathrm{I} = a(\sum\theta)^b$$

With I = the thickness of the ice, ∑θ = the total quantity of the daily negative temperatures and a, b being constants. A is equal to 1.33 and b = 0.58. [13]

The thickness of the ice will increase at a rate that is roughly proportional to the accumulated sum of the daily temperatures. This formula assumes that the ice forms in non-moving water and does not take into account many factors that could affect the rate at which the ice freezes. These include sea ice motion, snow coverage, sunlight and many other different surface conditions.

The factor that has the biggest impact on the rate of ice growth is snow coverage. This is because snow is an effective insulator and it also has a higher albedo than ice. This means the snow will slow down the rate of ice growth as it insulates the heat from the ocean.

Sea ice also grows in a small-scale vertical process. The rate at which sea ice is formed slows down when ice becomes thicker as it starts to act as an insulator. Heat from the ocean below must convect through the sea ice before being emitted into the atmosphere. During the freezing of ice, latent heat is released and conducted into the atmosphere. The thermal conduction in sea ice follows the Fourier law:

$$\frac{\delta}{\delta t}(\rho_i . c_i T) = \frac{\delta}{\delta z}(k_i \frac{\delta T}{\delta z} - Q_{s.i})$$

Where T is the temperature of the ice, c_i is the specific heat capacity, k_i is the thermal conductivity and $Q_{s.i}$ is the amount of solar radiation that is in the ice. The specific heat capacity and thermal conductivity are both constants. [13]

Due to temperatures in the Arctic dropping down as far as -33.3ºC in recent years [14] the ice will be very cold, meaning seawater can freeze when in contact with ice. When water changes state, it will stay at a constant temperature of 0ºC (32°F) until it has

completely frozen. Liquid water has more energy than ice which means that when liquid changes to a solid state, heat energy must be released, known as the latent heat of fusion. This heat energy must be carried away from the bottom of the ice to the surface before being released into the atmosphere for more ice to form.

The latent heat of fusion for ice is approximately 80cal/kg, and this could be substantial if a lot of ice is created. However, it's likely that for any ice formed on top of the surface, the heat produced will be radiated into space almost immediately. [4] This would still have an impact on the amount of ice that is formed, with any latent heat that is released potentially increasing the surface temperatures.

2.4.2 Thawing

In the summer months of the Arctic, temperatures increase by vast amounts due to the exposure of sunlight. Once non-existent in the winter months, sunlight provides a heat source to the area increasing temperatures upwards of 10°C. This solar radiation melts the surface of the ice, by how much depends on the albedo of the surface.

Data acquired from submarine cruises show that Ice has been thinning at an alarming rate. The thickness of ice has gone from 3.1m in 1958 to 1.8m in the late 90's. This shows that in 41 years the rate at which ice is thinning is approximately 4cm per year. This melting occurs mostly in the summer months and to combat this the loss of 4cm would need to be replaced. This would need to cover a huge area, so instead, the sea edges should be targeted. Increasing the thickness by 20cm is the target. [15]

There are other sources of heat that melt the Arctic ice as well. The sea water below the ice that has a temperature that is above freezing point also causes the bottom surface of the ice to melt. Both of these sources of heat, transfer energy to the ice and cause melting. The amount of heat required is defined as the latent heat of fusion, the heat to turn one gram of ice into a liquid water state without a change in temperature.

2.4.3 Electrical Properties

To be able to measure the thickness of ice it is important to know the electrical properties of water and how they change with temperature. Also, the salinity of water affects the properties so this too is an important variable to consider. The property needed to be found for water is its conductivity as the resistivity can be derived from it and hence resistance and conductance. Pure water has an almost negligible conductivity but can be quantified with the equation below. Where K is the conductivity of water, d is density (g/cm^3), λ_H^+ and λ_{OH}^- are the respective conductances of the hydrogen and hydroxide ions in the water and C_H^+ and C_{OH}^- are the concentrations of the ions. [16]

$$K\left(\frac{S}{cm}\right) = \frac{1}{\rho} = 10^{-3}d(C_H^+\lambda_H^+ + C_{OH}^-\lambda_{OH}^-)$$

There has been much research into the conductivity of water, specifically research done by Truman S. Light et al. in the "fundamental conductivity and resistivity of water", shows how the conductance of water changes with temperature. The graph in Figure 2.7 shows this data down to 0°C with the trend line continuing below 0°C. From this the change in resistivity is shown to be affected greater at lower temperatures.

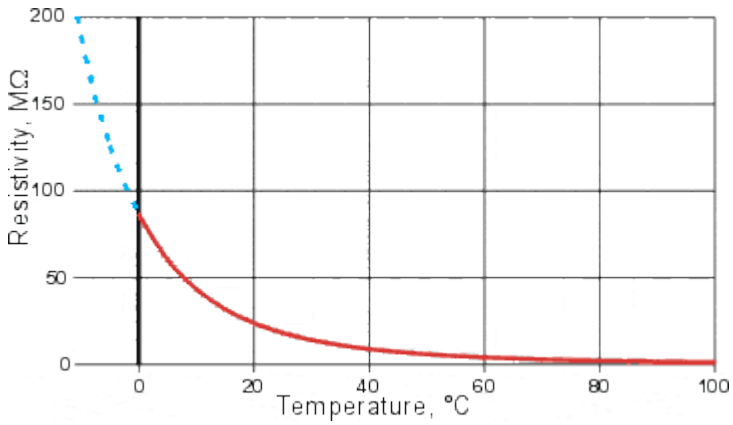

Figure 2.7 Resistive of water [17]

Impurities in water can change the conductivity; sodium chloride increases its conductance. The salinity of sea water varies from about 30ppt to 40ppt with arctic sea water at about 30-34ppt. Figure 2.8 shows how both salinity and temperature affects the conductivity of water. It clearly shows that the higher salinity levels cause a greater change in conductivity per degree change in temperature.

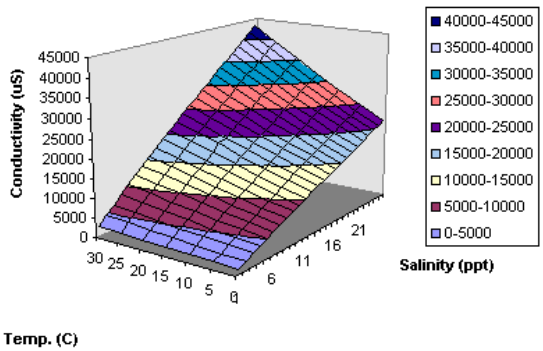

Figure 2.8 Conductivity of water against a change in temperature and salinity [18]

The Resistance measurement of water can have a more complex relationship than displayed in the above graphs. When a hydrophilic material is placed in the water the first layer of water is held strong to the surface of it. This can then change the apparent electrical properties of the water being measured and can give a negative resistance reading. This is shown in Figure 2.9, part a shows the normal ohmic conduction then part b represents the breakdown tunnelling with section c showing when a negative reading of resistance is produced. This negative reading for resistance is due to the electrolytic breakdown of the absorbed water. [17]

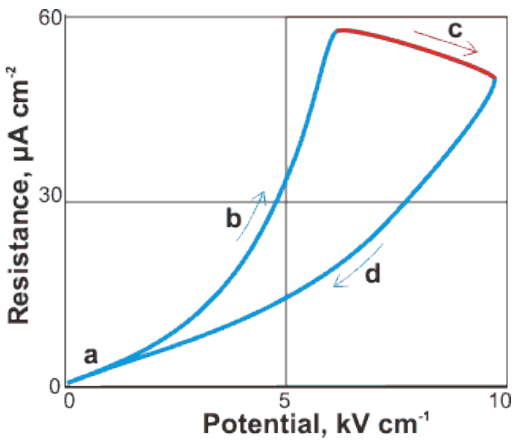

Figure 2.9 Resistance readings of water against an applied potential

2.4.4 Air Resistance

This project looks at distributing sea water over the surface of the Arctic to increase the thickness of the ice. To do this water must travel through the air before it reaches the surface which means it will be subject to an opposing force, air resistance. This force could have an impact on how far water can be distributed, with wind speeds also having

an impact on the water. The drag force acting on the water, especially if it was in the form of spherical droplets, could have a huge impact on the velocity of the water. The value of drag depends on several factors, and the equation is given as:

$$F_D = \frac{1}{2} pv^2 C_D A$$

Where p is the density of the air, v the speed of the object, C_D the drag coefficient and A the cross-sectional area of the object. [19]

The drag coefficient, C_D, is a value that is given to an object used to find the drag that it will face. A lower value means that the object will experience less aerodynamic drag compared to a higher value. The coefficient is not a constant, it depends on many different factors, and it can often be described as a function of the Reynolds number if the water was of the form of spherical droplets:

$$Re = \frac{Du}{v}$$

Where D is the diameter of the droplet, u is the relative velocity of the droplet and v is the kinematic viscosity of air.

If the water was distributed as droplets, then there would be an evaporation of droplets during flight. The volume of droplets would also decrease over time. The rate at which evaporation occurs can be modelled, with the total evaporation rate λ_t, equalling:

$$\lambda_t = \int_0^{D_{max}} \lambda_g f(D : P) dD \; x \; 100\%$$

Where f (D : P) is the value of the frequency function of the droplet diameter given P, the vector of the upper limit log normal distribution, which is found from the size distribution of the droplets and λ_g is the evaporation rate for a single water droplet. [20]

2.4.5 Laminar Flow

In fluid dynamics, laminar flow is when fluid travels in a uniform, parallel direction meaning that the fluid does not mix and undergo irregular fluctuations. Layers of water flow over one another without mixing whilst travelling at different speeds. This means the fluid can travel in a smoother motion without disturbances. Whether fluid flow is laminar or turbulent is determined by the value of Reynolds number.

$$\mathrm{R}e = \frac{pVD}{\mu}$$

Where p is the density of the fluid, V is the mean velocity of the fluid, D is the pipe diameter, and μ is the dynamic viscosity of the fluid.

Reynolds number is a value that shows the ratio between the inertial force and the shearing force of the fluid and can be used to predict whether the flow condition is laminar or turbulent. This value depends on several factors, the viscosity, the velocity of the fluid and the diameter of the pipe at which the fluid is flowing through. For laminar flow to occur, the pipe needs have a small inner diameter and the fluid needs to moving at slow speeds with a high viscosity. Laminar flow occurs in a circular pipe when the value of Reynolds number is typically less than 2300 [21]. This is often hard to achieve in many water systems.

When the value of Reynolds number is greater than 2300 and less than 4000 there is transitional flow. This flow is often unstable and is the transition between laminar and turbulent flow. The flow is unstable due to the onset of turbulence. Once the value is over 4000, there is turbulent flow which is when water particles will follow irregular movements and cause a disturbance.

In the project, water from the sea below the Arctic ice caps will be pumped and then distributed over the Arctic's surface. Before the water leaves the system, it will have to pass through several pipes. This is where achieving laminar flow could play a key role in trying to optimise the distance at which the water will travel.

2.5 Mechanical Actuators

2.5.1 Pumps

There are many types of pump that are used depending on their attributes for separate roles. The most common pump used in industry is the centrifugal pump. These pumps use an impeller driven by a shaft, that rotates at a high rate of 1750 or 3500rpm inside some sort of casing. Liquid is drawn into the suction inlet by the impeller and thrown against the walls of the casing, caused by the apparent centrifugal force that the water feels and then exits through the discharge port. This velocity that is transferred to the liquid by the impeller is then converted to pressure energy, defined as "head".

With the velocity being transferred to the liquid, both the pressure and the energy of the water will rise at the discharge end of the impeller. At the suction side, with water being displaced, a negative pressure is induced at the centre. This pressure helps suck fresh water back into the system again, continuing the cycle. Figure 2.10 shows a cross section of a centrifugal pump. The shaping of the casing displayed in the diagram clearly shows an increasing area in the direction of flow. This helps to let more water into the casing, but will also decrease the exit flow velocity. This reduction in velocity is required to increase the static pressure in the system, to overcome the resistance present in it. [22]

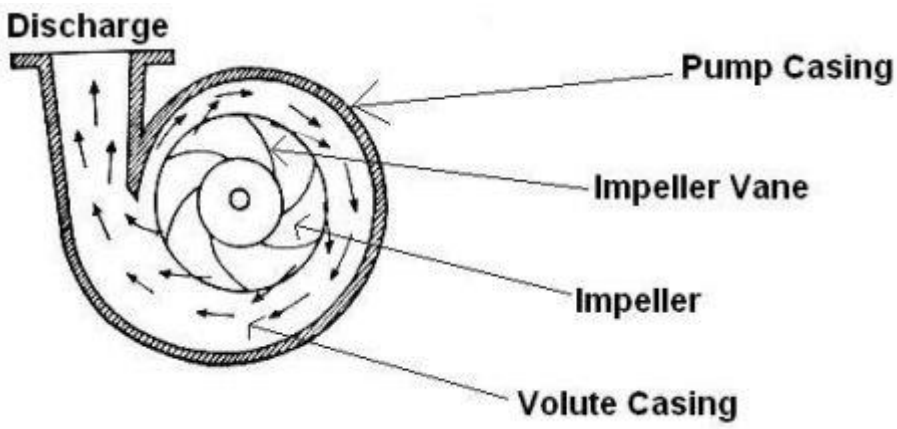

Figure 2.10 A cross section of a centrifugal pump. [23]

The efficiency of a centrifugal pump is normally defined as a series of curves on a graph that are effected by certain losses that the pump feels.

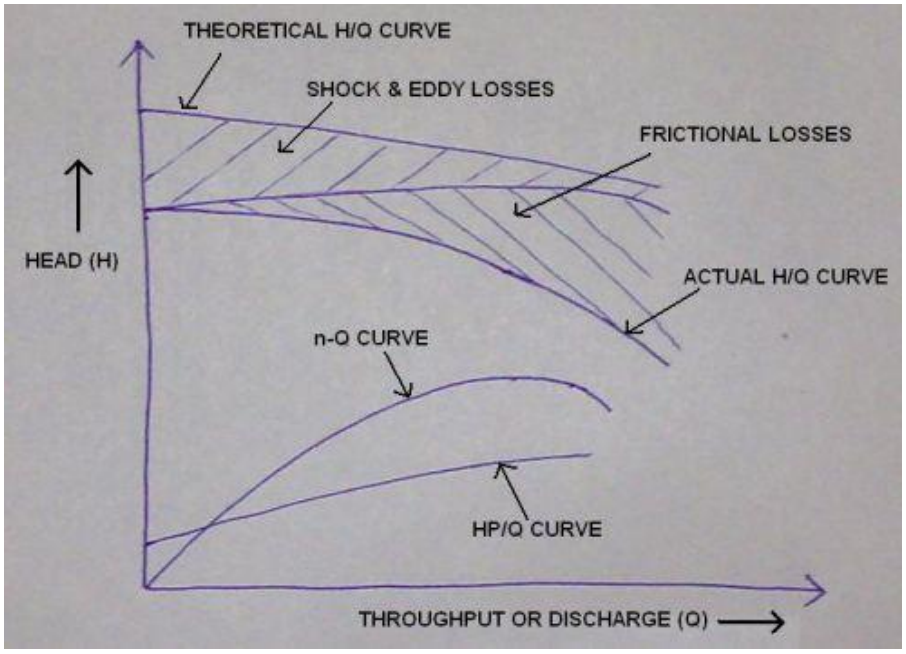

Figure 2.11 A graph of the performance characteristics of a centrifugal pump.

Figure 2.11 shows this with n-Q being the efficiency vs the flow rate and HP/Q being the horse power. In theory, the line of the head vs the flow rate is a straight line, as the top line on the graph shows. When there is no flow in the pump, the main loss of head is due to shock and eddy losses. Also, as the flow rate increases friction will create the most loss. This means that the actual H/Q curve is slightly lower than the theoretical one and shows a downwards trend as the discharge rate gets higher. [23]

The second type of pump that is commonly used in industry is a positive displacement pump. These pumps work by first trapping a set amount of fluid and then forcing it into a discharge pipe or a similar system. These types of pump utilise an expanding cavity on the suction side and a decreasing cavity on the discharge side. Liquid is bought into the pump as the cavity at the suction end expands and is pushed out of the discharge pipe as it collapses. This allows the volume inside the pipe to be constant throughout each cycle that the pump remains active.

Unlike centrifugal pumps, positive displacements pumps do not use impellers. Instead they utilise rotating or reciprocating parts that can directly push the liquid into the enclosed cavity until the pressure build up is high enough to push the fluid up the system. The downside to this is that the velocity of the fluid in the pump is much lower to that of a centrifugal pump. This does however mean that they can create a constant uninterrupted flow throughout their operational period. [24]

2.5.2 Motors

Motors turn electrical energy into kinetic energy by using magnetic fields. A coil of wire in a magnetic field as show in Figure 2.12 uses Fleming's right hand rule to demonstrate the effect the current passing through the wire. The opposite sides of the wire have an opposing torque on the wire which is the force that turns the output of the motor.

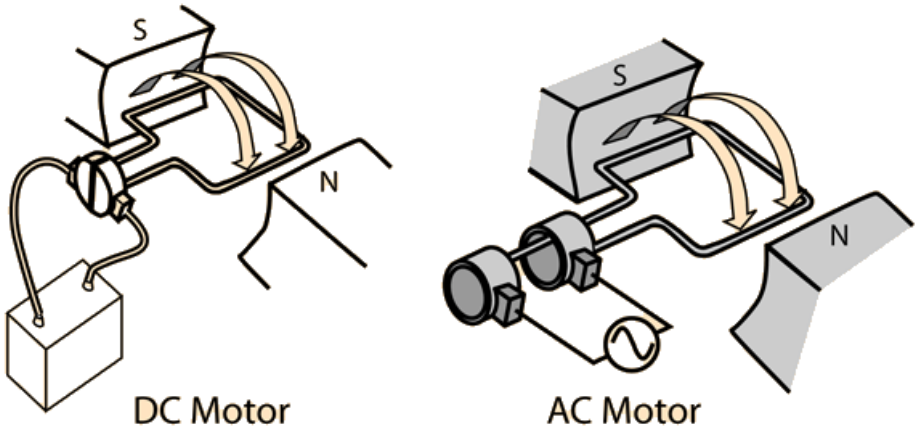

Figure 2.12 Motors [25]

Figure 2.13 shows the development of the motor. Additional wire loops are added to balance out the torque of the motor and the magnets are changed to electromagnets.

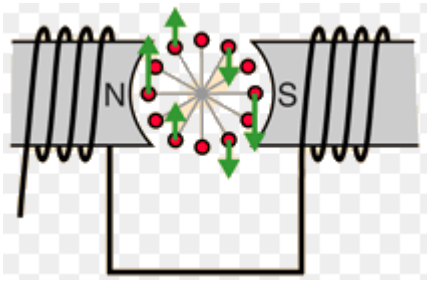

Figure 2.13 Advance of the motor [25]

2.6 Inuit Population

In Northern Canada, there is an Inuit population that could be used to maintain and deploy the final design. The Inuit people are situated in 3 major areas, Inuvialuit, Nunavut and Nunavik. Research into the wind speeds was done in an area around the Baffin province in the Nunavut area, therefore further investigation was done to determine what populated areas there may be and whether they would be willing to help.

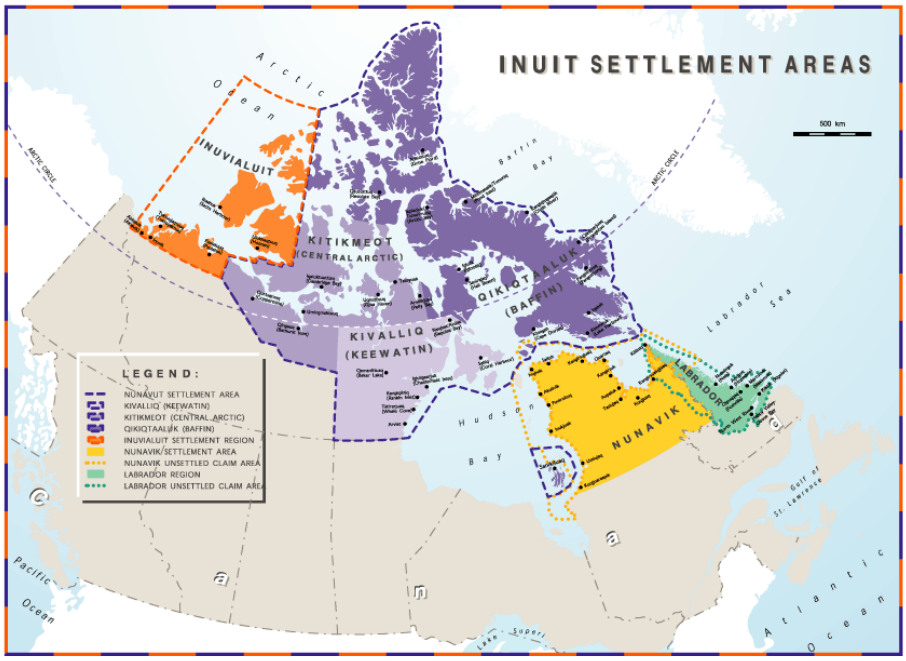

Figure 2.14 A map of the area that Inuit inhabit in northern Canada. [26]

The population in these areas is rather small, as of July 1st, 2016 there was a total of 19,654 people, of which 13,127 are of working age (between the ages of 15 to 64) in the Baffin region. The closest population area to which wind data was obtained was Resolute, a tiny town with a population of only 210, of which only 145 are of working age. [27] There are a few areas that have larger populations, but these are mainly below the arctic circle line, with only a few being above it. There should, however, be enough people to help maintain the project and who might be willing to work. Data shows that the Inuit population are considerably worse off compared to the rest of the Canadian population, therefore any jobs that could be offered in areas which they already in are proficient in, that is the maintenance of mechanical components, would go a long way in minimising that gap. [28]

2.7 Literature Review

Interest in this area of research is ever increasing, with the Arctic Ice reducing in size at an alarming rate but with few solutions being thought of. Many researchers are simply put off by the size of the ever-growing problem, the huge costs involved and the huge amount of resources that would need to be used. However, there are some exciting papers being published that could provide useful and helpful information for this project.

The paper, "Arctic Ice Management" [29] was published 24 January 2017 and proposes a similar idea to this project in an attempt to propose a solution to the shrinking Arctic. The paper mentions that "it is likely that the late-summer Arctic will be ice-free as soon as the 2030s", which shows the importance of trying to come up with an achievable solution. This loss of sea-ice would potentially cause many problems, with no sea-ice less sunlight will be reflected into the atmosphere. Due to the sea-ice albedo effect, a decrease in ice will increase the rate at which the ice is melting. The study also mentions that "it is unlikely that CO2 levels and mean temperatures can be decreased in time to prevent this loss, so restoring sea ice artificially is an imperative", which proves the huge importance of trying to come up with a solution.

Also, this study proposes a wind-powered pumping device that would "pump roughly 1.3m of water over the course of the Arctic winter". This is a similar proposal to this project, but the idea is to pump more water than the 20cm planned. For this to work however, there must be a consistent amount of wind to provide enough power for the pumping device. The paper mentions that "the average wind speed over the whole Arctic is 6.4 ms^{-1}" which is more than enough wind to provide the necessary power. This further proves that wind is a viable option for the source of power.

This paper suggests that the device will be "mounted on a large buoy" and it will capture wind energy in order to pump and distribute water over the Arctic's surface. This is a different approach, with this project looking at pumping from a hole made in the ice sheet. Furthermore, the paper suggests that a vast number of devices will be needed over the Arctic's area. The study says that "If wind-powered pumps are to be distributed across 10% of that area, this would necessitate about 10 million wind-powered pumps'. This is a massive number of devices, and this comes with astronomical costs. The paper suggests that "to deploy the devices over 10% of the Arctic in 10 years would require about $50 billion per year", which is an unfeasible cost for only 10% of the Arctic's area. [29]

Many different sources were also analysed to come up with a good idea to measure the thickness of sea ice. A book named, “Field Techniques for Sea-Ice Research” [30] had some useful information on measuring the sea ice using EM sounding. Here a transmitter coil would create a primary electromagnetic field, this in turn would generate eddy currents in the conductive sea water below the ice. This generates a secondary field for which a receiver coil would measure the strength and phase of this field.

Furthermore, the paper “Freshwater Ice Thickness Apparatus Based on Differences in Electrical Resistance and Temperature” [31] was also looked at. This shows a way of measuring the thickness of ice, taking advantage of the different electrical resistance of ice and water. Here two stainless-steel screws would be used as fixed electrodes in the ice, one detecting and one returning electrode. The resistance will be measured at both electrodes and compared using a multiplexer. This type of method for measuring ice thickness is also shown in the book “Field Techniques for Sea-Ice Research” and was deemed to be the best way of measuring Ice.

Chapter 3: Research and Further Reading

3.1 Arctic Weather

The weather in the Arctic is heavily going to impact the ability of this project to operate properly. The design will need to operate in low temperatures and cope with whatever wind speeds that may be present, whether they be high or low. Research was done in finding a weather station in the Arctic Circle that could give some insight into the type of conditions that might come to be expected.

3.1.1 Wind

With one possible way of powering the device being wind energy, the amount of wind available in the Arctic is very important. In one of the papers explored in the literature review, Desch et al. published a paper entitled "Arctic Ice Management" [29] which explored ways to manage the ice in the Arctic. In this paper, they show the average wind speed in the Arctic circle, shown in Figure 3.1 and discovered that the average wind speed in the area was equal to about 6.4 m/S. This data takes into account a large area, but the main area that is of interest in this project is that where the Inuit peoples reside, Northern Canada.

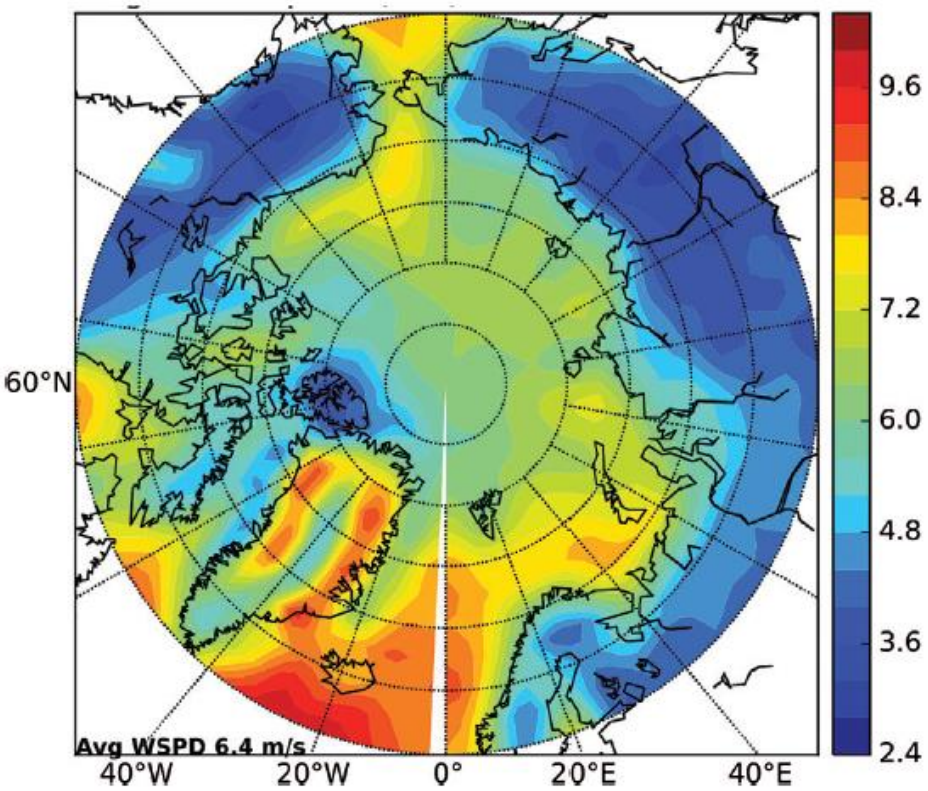

Figure 3.1 Wind speeds in and around the Arctic Circle in m/s,

Upon further investigation, a small research station was found in Northern Canada called Isachsen. It is located on the western shore of Elles Ringness Island in the Sverdrup Islands and used to be a joint weather station with Canada and the US. It has been unmanned since 1978 but in 1989 an automated observation system was set up to allow the weather to be monitored remotely. Meteoblue holds wind and temperature data for the site all the way back to 1985 and using this data an idea of the wind that would be available for the design was developed. The data gathered included the wind speed at the height of 10m above the ground and using this data an average was obtained for the winter months, equal to 4.86m/s. The percentages that the wind speeds were are 2m/s, and 5m/s were also investigated as these are generally the cut in speeds for wind turbines. This produced the graph shown in Figure 3.2 which shows that the percentage of time that the wind was at 5m/s to be about 42% in 2010-2015, and the percentage of the time the wind was at 2m/s to be much higher at 82%. This provides a strong indication of the types of wind speeds that might be encountered in the area in and around Isachsen, and therefore good benchmarks for the requirements of any wind turbine that might be operable in the area.

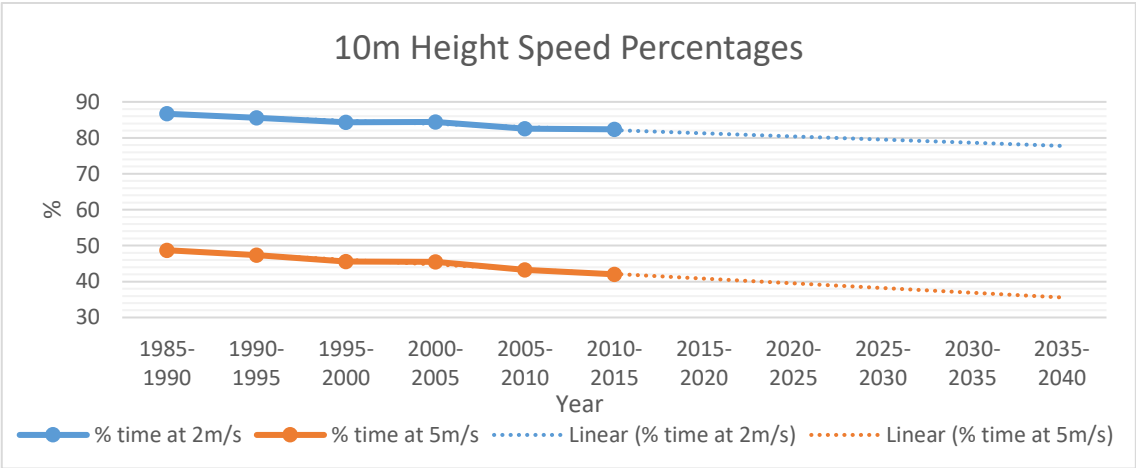

Figure 3.2 A graph showing the percentage that wind speeds occur in the Arctic at the height of 10m

Another area of interest was the direction that the wind blew. Knowing this could decide where the wind turbines should be situated depending on what types of wind turbine were to be used. Figure 3.3 shows a wind rose which shows the most common direction that the wind blew was NNW.

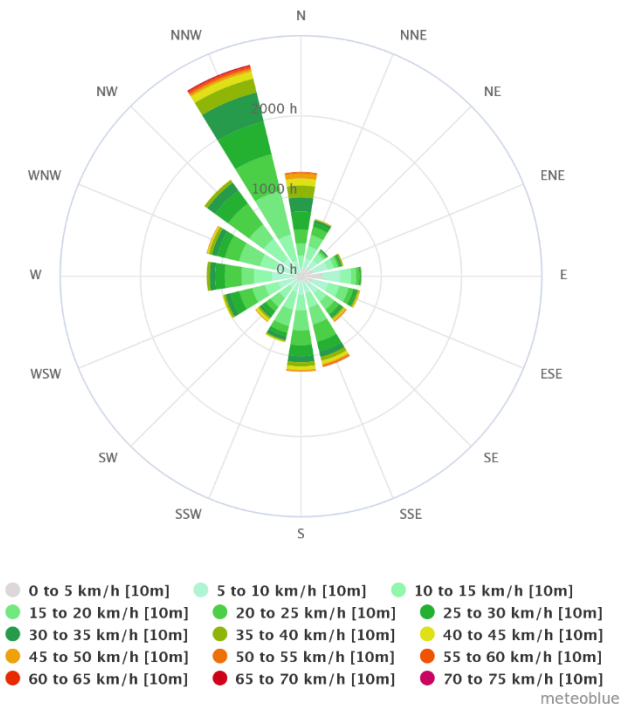

Figure 3.3 A wind rose of the direction the wind blew in the year 2016

3.1.2 Temperature

Included in the data that Meteoblue provided was temperature data. As the main interest for the project is the winter months, this was the time that was investigated. Over the last winter, November 2016 to February 2017, the lowest temperature was -33.3°C and the highest -7.2°C. The most common temperature that the station experienced was -30°C, but the average across the entirety of the winter was -23.7°C. These temperatures are a good indication of what any device that is to be placed in the Arctic would have to cope with. [14]

3.2 Energy Requirements

The system proposed in this project requires a certain of amount of energy to function and perform as designed. The energy is needed for the pump and motor which will be produced using a wind turbine. The pump required 165.6W to work at its full potential and the motor 100W, meaning the entire system would only need 265.6W to function.

3.3 Power Generation

3.3.1 Wind Generation Systems

Using wind turbines was thought as the most efficient way of extracting power in the Arctic. As mentioned in section 3.1.1 in the winter months the average wind speed depends a lot on location. The data gathered from a small island, Isachsen, in Northern Canada has an average speed of 4.86m/s. However, the paper entitled 'Artic Ice Management' [29] mentions that the average wind speed of the Arctic is nearer 6.4m/s. This value considers a larger area rather than once specific place such as in Isachsen.

3.3.1.1 Horizontal Axis Wind Turbines

Horizontal Axis Wind Turbines (HAWT) are the most common type of turbine and they have a rotating axis which is horizontal or parallel with the ground. On the large scale, they are used a lot more than VAWT's due to them being able to produce electricity in larger quantities with a given wind speed. However, they have certain properties for which they were deemed unsuitable for this project. The turbines are generally quite heavy and very loud. Also, due to the projects requirements of a mobile system, using a large heavy turbine would not be possible. Furthermore, in the Arctic conditions are very harsh and there are often turbulent winds. Horizontal turbines do not perform well in turbulent winds which is another reason the turbines were discounted.

3.3.1.2 Vertical Axis Wind Turbines

Vertical Axis Wind Turbines (VAWT) are different to HAWT's as there axis is vertical or perpendicular to the ground. They are primarily used on small scale projects and for residential applications. The turbines, due to their vertical axis, have the ability to produce power from wind even in tumultuous conditions. So, because wind conditions in the Arctic are not consistent, VAWT's would work a lot better than the horizontal counterparts. For this reason, VAWT's were looked at to be used for this project.

The wind turbine that was provisionally used for theoretical purposes was the Helix-Wind turbine: Wind of Change. This turbine has a height of 2.1m and a diameter of 1.4m. It was provisionally chosen because of its low cut-in speed of 1.4m/s. The system is lightweight and robust, practically silent, can handle wind speeds of up to 24-27m/s and temperatures of down to -35°C. These are all good characteristics required to handle the harsh Arctic conditions. In addition, the turbine has a power coefficient of approximately

50%. This means that the power that is available to the rest of the system once the turbine has converted the wind can be calculated. The power produced is:

$$\mathrm{P} = \frac{1}{2}\, pAv^3 * C_P$$

Where p is the air density, A is the area, v the wind velocity and C_p is the power coefficient of the turbine. This means for speeds of 4.86m/s the amount of power available will be equal to about 373W. If the average speed is upwards of 6.4m/s, as mentioned in [29], then there will be approximately 852W available for the device. This is more than enough power for the entire system to run on.

3.3.1.3 Pole

Vorticity is the curl of the velocity field within a fluid and measures its local rotation. This equates to how likely the fluid is to spin [32]. Absolute vorticity is defined as.

$$\omega_a \equiv \nabla \times U_a$$

Relative vorticity is defined as.

$$\omega \equiv \nabla \times U$$

This gives a value for ω as.

$$\omega = (\frac{\partial \mathrm{w}}{\partial \mathrm{y}} - \frac{\partial \mathrm{v}}{\partial \mathrm{z}}, \frac{\partial \mathrm{u}}{\partial \mathrm{z}} - \frac{\partial \mathrm{w}}{\partial \mathrm{x}}, \frac{\partial \mathrm{v}}{\partial \mathrm{x}} - \frac{\partial \mathrm{u}}{\partial \mathrm{y}})$$

Vorticity is important as an experimental form of wind power generation. A wind generation system that uses this effect is currently being developed by Vortex Bladeless [33]. Figure 3.4 shows the effect of the wind on the cross section of the turbine. There is a critical velocity of the wind where vortices form on alternating low pressure zones, these cause the turbine to oscillate perpendicular to the direction of the wind. The term for this phenomenon is defined as vortex shedding. It can cause other cylindrical structures to oscillate when they are not designed to, but this design of bladeless turbine uses this effect for power generation. Figure 3.5 shows the physical structure of the turbine. With no blades and the only moving parts being the structures oscillation, the noise pollution associated with traditional turbine design is removed. The turbine is 30% less efficient than a similar sized wind turbine but being bladeless they can be packed twice as close together. This means that per square feet the energy collected is 40% higher

than a traditional HAWT. Unfortunately, this design is still under development and therefore unfeasible to use in this project.

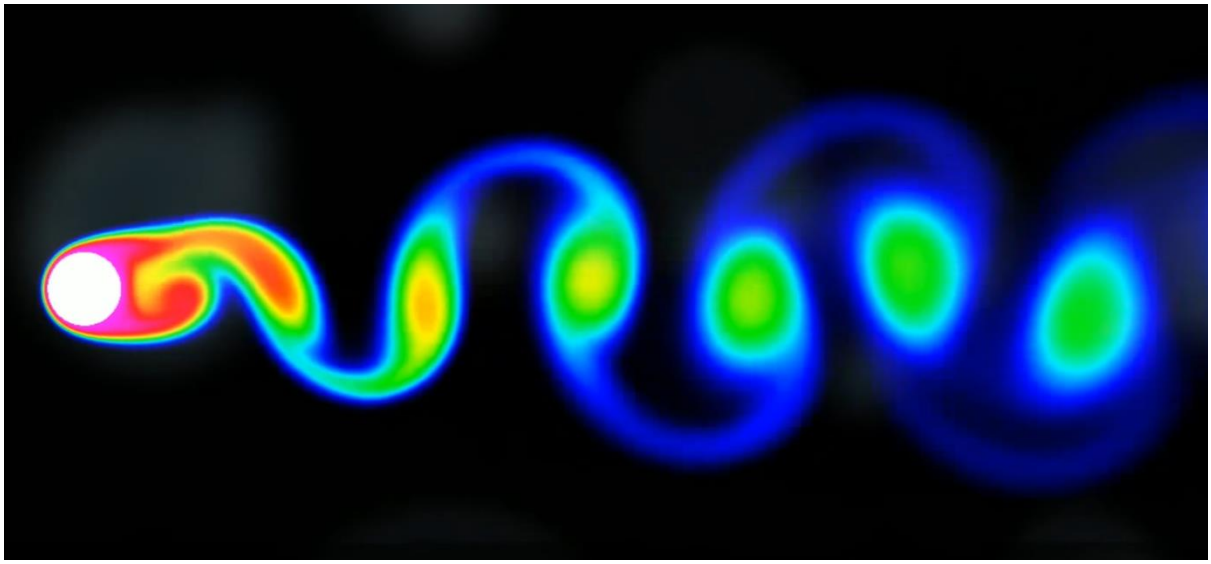

Figure 3.4 Vorticity Effect on Bladeless Turbine [34]

Figure 3.5 Bladeless Turbine [35]

3.3.1.4 Kite

Another way that could be used to generate wind power is a kite system. These systems allow a user to harvest wind power at a higher altitude than a normal turbine, the concept being to use wings or power kites which are tethered to the ground by two ropes. This allows these wind turbines to reach a height of 800-1000m above the ground. The theory

is that at higher altitudes, there are stronger winds that are a lot more frequent than they are on the ground. This allows the kite to operate a lot more often and at better efficiencies than a wind turbine might achieve at a lower altitude where there is less wind. The flight of the kite is tracked using wireless instruments on board that communicate the information back down to the ground. Once the data is received, an automatic control unit maintains its altitude and the motion of the kite. The kite generates electricity at the ground level by converting the traction forces that are acting on the wing into electrical power. It does this using rotating mechanisms and electric generators, shown in Figure 3.6. [36]

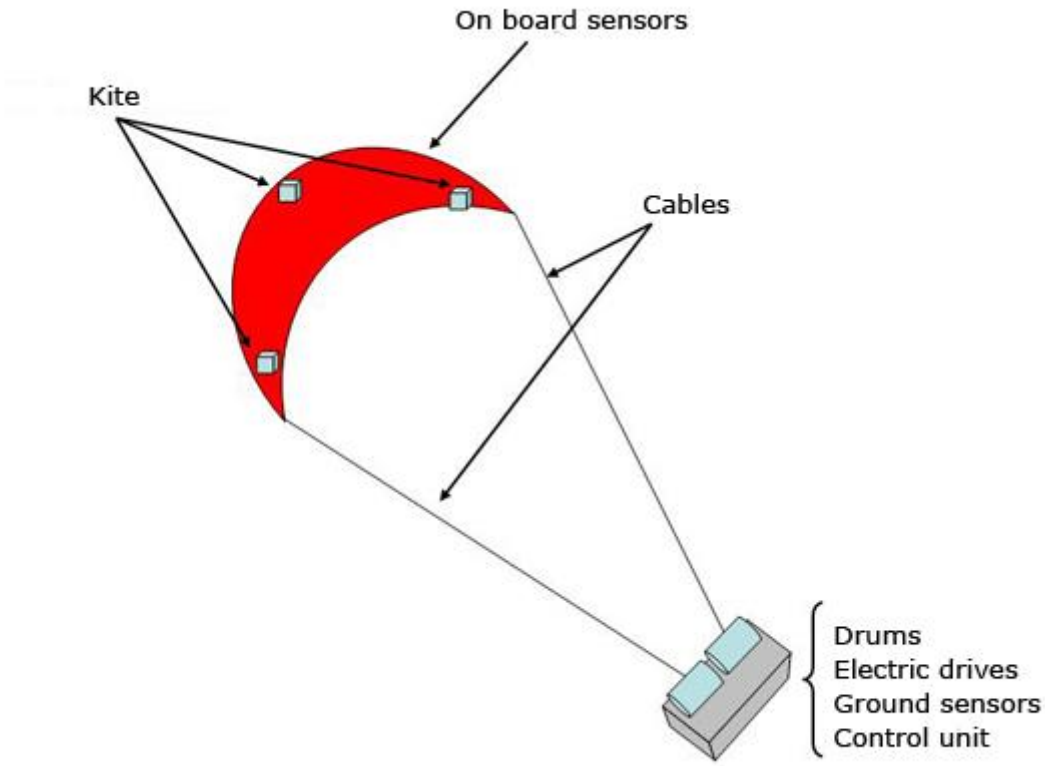

Figure 3.6 A typical kite system used for power generation

After investigation into the kite idea for electricity generation, it was decided that it would not be a feasible design to use due to the very slight differences in wind speed observed at higher altitudes compared to lower at ground level.

3.3.2 Peltier

The Peltier relies on the thermoelectric effect where a voltage is converted into a temperature difference or a temperature difference is converted into a voltage. A thermoelectric device when a voltage is applied has a cold and a warm side. This method

of power generation has the possibility of creating power by using the ice and the surrounding environment to create the required temperature differences. In this project the outside air will be the hot side and the ice will be the cold side producing the temperature difference required for the Seebeck effect to occur and create electricity. However due to the temperature difference between the ice and the water, the amount of power produced would not be large enough for this to be a worthwhile way of powering the project.

3.3.3 Water Turbine

The limitation of water turbines in this project is the lack of moving water that is required. Furthermore, a hydroelectric generator style arrangement will also be impossible due to the flat nature of the Arctic and no possibility of building such a permanent structure. Due to these reasons, water turbines will not be used as a power generation method in this project.

3.4 Water Manipulation

With the design relying so heavily on the manipulation of water to succeed, many ways of extracting it from underneath the ice sheets had to be researched, as well as ways of distributing it so that it reaches as far as possible above the ice.

3.4.1 Water Extraction

3.4.1.1 Pump

One of the key features of the design is the pump that draws up the water from underneath the ice. One of the first ideas for the project was to use a kite to draw up a bucket of water. The aim of the kite would be to draw up 60l of water each time, which would require a design to have a coefficient of lift somewhere within the range of 0.2 and 1.5. In the Arctic, with a kite that had a wing area of 42 square metres, the coefficient of lift generated would be somewhere between 0.79 and 0.93, which is within the required amount, making it possible to lift the 60l of water. Once it is brought to above the ice however, it would still be required to be distributed by some form. For that reason, it was decided that using a traditional pump would be required.

Due to the requirements that such a pump would have to have a high flow rate, a centrifugal pump would be the best choice for the design. From looking at the pumps currently available on the market, the best type of pump available is a bilge pump. These pumps typically operate on boats, drawing out any water that has got into the hull and depositing it back into the sea. The pump chosen for this design was the Rule 4000 electric submersible pump. This pump operates at 24v and produces a flow rate of 15140lph at a 0m head. The submersible nature of the pump allows as much of it as possible to be placed inside the water, limiting its contact with the ice, and therefore the chances of it freezing over and requiring maintenance. The low voltage of 24v coupled with its amp draw of 6.9amps means that one of these pumps only requires 165.6W of power. [37] This is almost half of the power made available by the proposed Helix-Wind turbine; Wind of Change explored in section 3.3.1.2, meaning that it may be possible to use two of these pumps to double the available output.

The only downside of using these types of pump is the low head that they provide. The proposed pumps flow rate drops off drastically at increasing heights shown in Figure 3.7

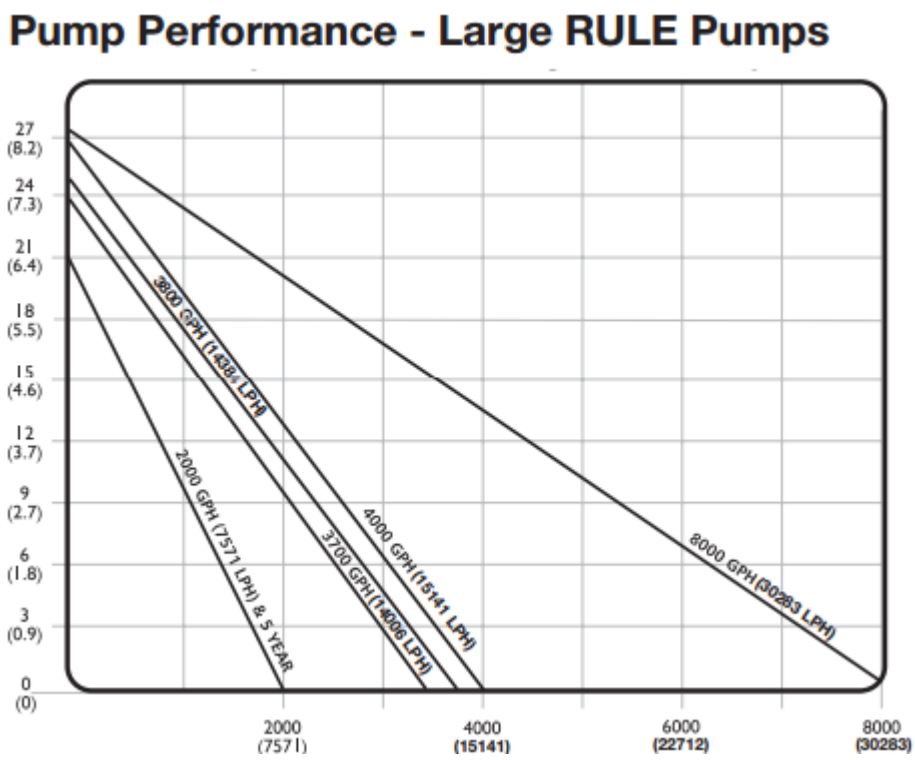

Figure 3.7 Rule 4000 pump performance

As this is the case, it may be desirable to find a pump that can produce high flow rates but at a much higher head. On the current market however, no such pump exists that can operate to the required power and flow specifications. Everything available either has a high head and low flow rate or the opposite. A pump that operates exactly to what is required will either need to be specifically ordered or technology must increase to such a point that what is required is directly available on the open market.

3.4.2 Water Distribution

3.4.2.1 Sprinklers

The first idea that was looked at for the distribution system was sprinklers and irrigation systems. These seemed suitable due to them being specifically designed to distribute water over a large area. Many different sprinkler systems were looked at, with some sending water over a 150ft radius. However, in the Arctic temperatures can reach down to -40^{0}C which would have an enormous impact on a sprinkler system. The harsh conditions would freeze a sprinkler system causing blockages in the pipes and head of a system. To prevent this, huge amounts of energy would need to be assigned to the system, energy which isn't available.

3.4.2.2 Helicopter

The final idea that was suggested was the use of what was dubbed the "helicopter hose" design. This design utilised a set of spinning pipes that increased the exit velocity of the water, therefore furthering the distance the water travelled. It does this using the mechanics of centripetal force. Centripetal force states that any curved path that represents a constant acceleration requires a force towards its centre to keep it on the curved path. This is called the centripetal force and is defined by the equation below:

$$F = m\frac{v^2}{r}$$

If there is no force to hold an object spinning on the curved path towards the centre, then it will travel off in a straight line tangential to that of the curved path. This means than from the perspective of anyone looking at the object it seems like it has experience another force, or a "centrifugal" force pushing the object outwards away from the curve.

In the design process, this "centrifugal" force was used to increase the velocity of the water exiting the pipe. Calculation of the theatrical max velocity that could be achieved was done using the height of the apparatus, the length of the pipe and the angle that the pipe was at. Due to the maximum head on the pipe, the amount of water it outputs at greater heights decreases based on the line shown in Figure 3.7. All of this data was inputted into an excel spreadsheet and using the radius of the output pipe, it was possible to theorise that the maximum possible output velocity was 2.68m/s.

Using this exit speed, it was possible to estimate what the speed of the water would be if it was spinning. The exiting of the water creates a vector going upwards at an angle of 45° from the perpendicular, shown in Figure 3.8 below by the blue arrow. The rotation of the pipes creates a separate vector, shown as the red arrow. The combination of these vectors is shown by the orange arrow.

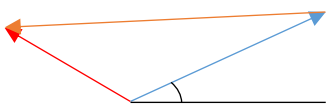

Figure 3.8 The vectors present in the design

This means that the final output velocity of the water will be equal to the equation below, where V_e is the exit velocity of the water, V_r is the rotational velocity of the system and θ is the angle that the pipe is at.

$$V_f = \sqrt{(V_e * \cos\theta)^2 + {V_r}^2 + V_e * \sin\theta}$$

This means that if the exit speed of the water before spinning is 2.68m/s and the system begins rotating at 50rpm, which is equal to 5.236m/s, with the angle of the pipe being 30°, then the new exit velocity will be equal to 7.07m/s. This represents an increase of 263% in the output compared to when only the pump is operational.

The use of a "helicopter hose" allows the system to be in constant movement, mitigating any effect that the extreme cold has on the system. With the increase in the exit velocity for a smaller increase in power usage, this plan represents a very good way of spending the energy that is available.

3.5 Instrumentation

3.5.1 Inputs

3.5.1.1 Wind Speed

Measuring wind speed for this project is important as the wind powers all electronic components including the pump and the control systems to manage the unit. Measuring the wind speed can be useful as it can be compared to the wind turbine output to measure efficiency and status of the wind turbine. If the wind turbine has suffered a failure, alerts to the notification network can be made to notify the operator. Dangerous wind speeds can affect the safety of the unit, and therefore the wind speed can allow the unit to detect and then protect itself when weather conditions become unfavourable. Wind speed measurement is done using an anemometer this uses a blade turbine to trigger an input into a circuit which is then calibrated against known wind speeds accurately. Cup anemometers are a common anemometer type where the cups as shown in Figure 3.9 are directly attached to a motor which acts as a generator when rotated which in turn creates a current.

Figure 3.9 Cup Anemometer [38]

Another method is to use a turbine with magnetic elements in the blades as shown in Figure 3.10, therefore when spinning a hall effect sensor placed near the unit will pick up the changes in magnetic flux density, the output is then fed into the control systems which once calibrated can accurately calculate the wind speed. For ease, a prebuilt anemometer that has already been calibrated to measure the accuracy of the wind speed was bought. Figure 3.11 shows the inside of the anemometer which uses a hall effect sensor, four pins in the corner of the PCB allow access to the wind speed data using serial.

Figure 3.10 Hall Effect Anemometer

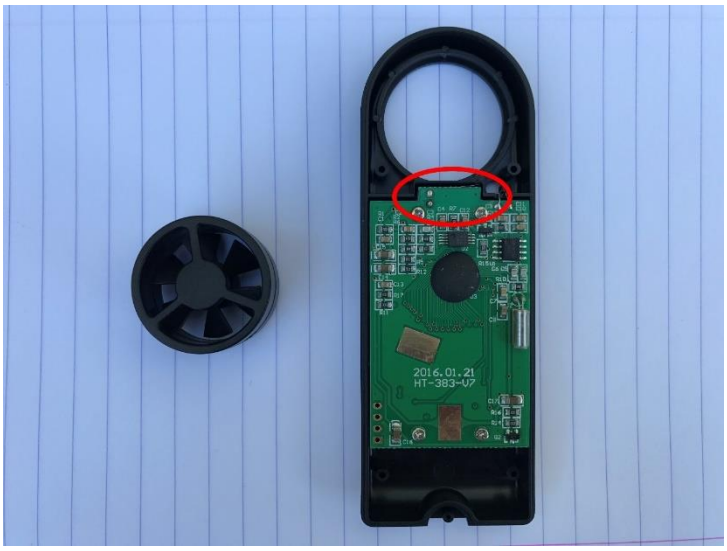

Figure 3.11 Magnetic turbine with hall effect sensor

In addition to the use of wind speed measurement systems that use physical mechanisms as their detection methods, non-contact methods were also investigated. These include an anemometer that uses ultrasound to get its readings. After some research, a schematic was found that could be easily integrated into the current instrumentation. Ultrasound works using a very high frequency sound and bouncing it between two transmitters and receivers. One key factor to consider when using this method for detection is the change in the speed of sound due to the temperature. As there will temperature sensors on the unit the below formula can be used to calculate the speed of sound at the current temperature, $C(^{m}/_{s})$.

$$C(^{m}/_{s}) = 331.3 + (0.606 * T(°C))$$

This design uses two transducers that are set to be 0.36m apart from one another. If there is a wind going between one of the transducers to the other, the time taken for the wave to travel to the other will vary depending on the direction of the wind. If there are two transducers, one in the north and one in the south, and there is a wind speed of 1kph going from north to south, then the time of the flight is going to be equal to 0.36/(317.88 + 0.277) = 1131.5µs, and from south to north it will be equal to 0.36/(317.88 - 0.277) = 1133.4µs. With no wind the time will be 1132.5µs, meaning that there is a difference of between 0.9µs and 1µs with 1kph of wind present. This means that any method that measured the wind speed at the required resolution would have to be able to measure a flight of at least 1ms.

This design uses an Arduino to calculate all the necessary time delays as well as using hardware. All the necessary coding and information as to how to build and design this system was found on an Arduino forum and a source forge page. With further investigation it would be possible to recreate and tweak the design so that it would function as is needed for the project, but with the limited time frame it was not possible to do anything with the information that was gathered. [39]

3.5.1.2 Ice Thickness

To aid with experiments and with the full-scale unit in operation, being able to measure the thickness of the ice as it grows and melts is key. To do this, there are several methods that can be approached each with their benefits and drawbacks. There are two main ways of measuring, non-contact methods and contact methods.

Firstly, looking at the contact methods one design is to use a rod with a plate on both ends that would go through a hole in the ice just bigger than the rod. It would then move up and down until the plates meet the ice and it would be unable to move any further. The movement of the rod could be controlled with a servo, geared stepper motor or solenoid. The displacing of the rod in both directions could be measured by the control method or as feedback from an optical sensor. The distance travelled by the rod can then be used to give the ice thickness. Figure 3.12 shows how the device would operate. There are drawbacks of this as the rod could freeze and get stuck in the ice and when the ice is very thin, it could break through.

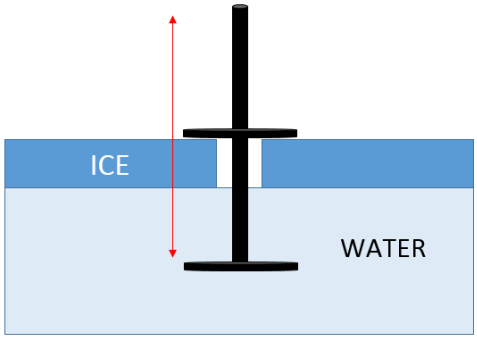

Figure 3.12 Sensing Rod Design

Another contact method is to use two parallel plates a fixed distance apart with several electrodes as rows across them as displayed in Figure 3.13. This would be placed on the surface of the water, and the water would freeze between the plates. The resistance or conductance would be measured between each plate and from this, the thickness of the ice would be able to be calculated as it is known that the conductivity and hence resistivity of water changes with temperature. The advantages of this method are there are no moving parts to freeze, and it can easily be scaled up. However, it will only give the ice thickness in one spot as it cannot move once frozen but several of these could be used.

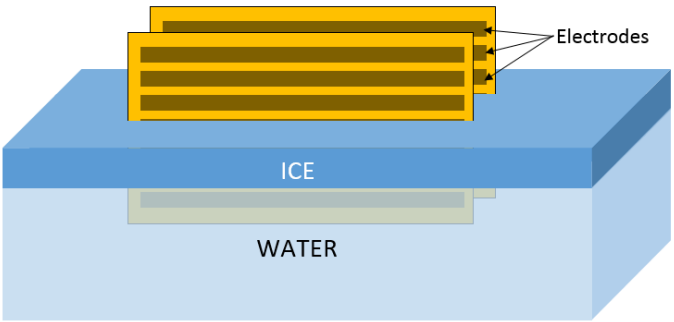

Figure 3.13 Parallel Electrode Plates

Another method of utilising the measurement of conductance is to place electrodes along the top of the ice and measure between them. With the electrodes a known distance apart, the conductance measurement can be used to give the ice thickness. This method would require the electrodes to be constantly repositioned to the surface of the ice as it grows.

Using non-contact methods has a key advantage over contact methods of measurement in that they will not interfere with the ice as it grows and melts. One way to do this in the small-scale experiments would be to have a camera looking at the side of a clear tub in a freezer with markings a known distance apart on the side. With LEDs to light the inside there would be a clear line between the bottom of the ice and the water, software can be used to then calculate the ice thickness. Figure 3.14 shows an image of this with the line between the ice and water clearly shown. However, this method could not easily be used on the full scale in the Arctic as it needs to have a side on external view of the water.

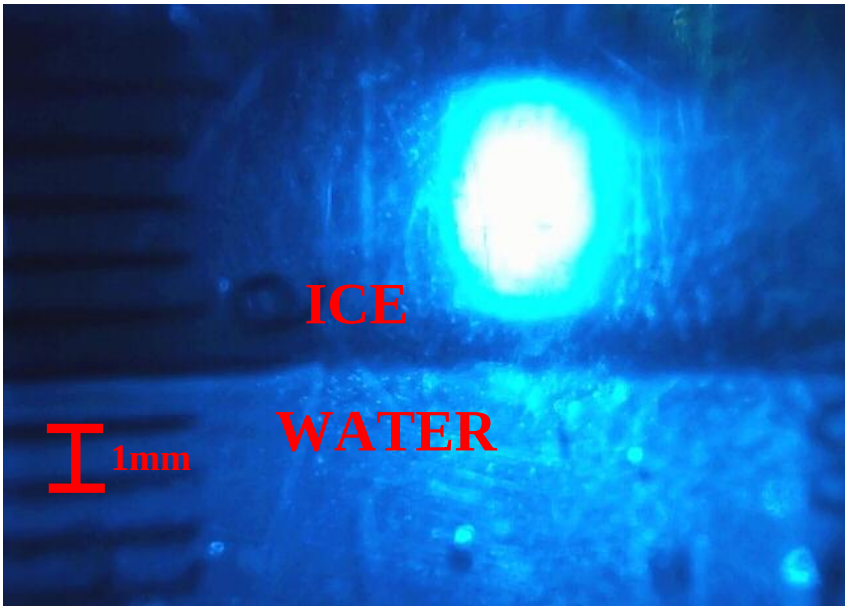

Figure 3.14 Macro View of Ice in a Transparent Container

Another method is to use two ultrasonic range finders above and below the ice. It cannot be done with just one as the ultrasonic wave will not easily transfer from one medium to another. Figure 3.15 shows how they would be set up, the waves from the upper sensor would travel through the air and reflect off the surface of the ice. The waves from the lower sensor would travel through the water and reflect off the bottom of the ice. With the sensors a fixed distance apart the time taken for the wave to travel from the sensor and reflect can be used to calculated the thickness of the ice. There are disadvantages of this method, one being that it would be unable to differentiate between water and ice on the surface and waterproof sensors with a high resolution are expensive < $150 [40].

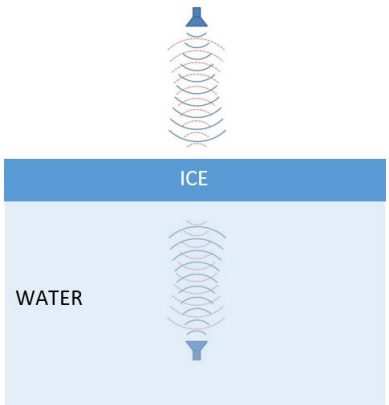

Figure 3.15 Ultrasonic Ice Thickness Measurement

A Raman LIDAR can be used with a spectrograph to measure ice thickness; Figure 3.16 shows how the setup would work. The lens would adjust to change the position of the laser beam waist. Water and ice give different Raman spectra that can be used to identify where the bottom of the ice is and elastic scattering can be used to find the top of the ice. [41] The major issue with this is that it requires very expensive equipment and for this cost, the resolution is no greater than some of the other cheaper methods.

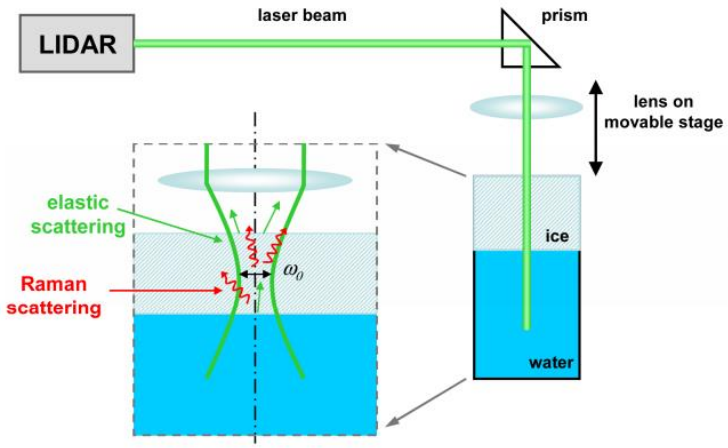

Figure 3.16 Raman Scattering Ice Thickness Measurement [41]

Due to air, water and ice having different refractive indices the reflection/refraction angle of a laser could be used to measure ice thickness. A line of photodiodes could be used to pick up the position of the laser after it had to be displaced by the ice. Using total internal reflection with a setup similar to the ultrasonic method with sensors above and below the ice would not be practical. This is because the critical angle of water to ice is roughly 80° as their refractive indices are very close, 1.33 and 1.31, in turn, this would mean the width of the sensor would have to be over 5 times the thickness of the ice to be measured. The other way to implement this is to shine a laser up from the water towards the ice at a much smaller incident angle, so the light is refracted. As the thickness of the ice changes the position of the laser above the ice moves along an axis perpendicular to this as depicted in Figure 3.17. When testing this concept, it was found that the rough and unpredictable surface of the ice caused the light to scatter for unreliable results.

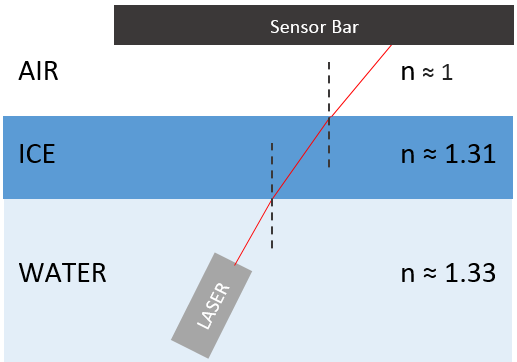

Figure 3.17 Refraction Based Ice Thickness Measurement

As was mentioned briefly in section 2.7 another way to measure ice thickness is to use electro-magnetic sounding. Figure 3.18 shows how this operates, a transmitter coil produces an electric field that induces an eddy current in the salt water below the ice. This in turn induces an electric field that is picked up by the receiver coil. The distance Z_E is calculated depending on a change in amplitude and phase of the received signal. This method is commonly used to measure ice thickness over a very large area by attaching it beneath a helicopter. It would not be able to be done for the small-scale experiments as the metal walls and motor inside the freezer would interfere with the EM signal.

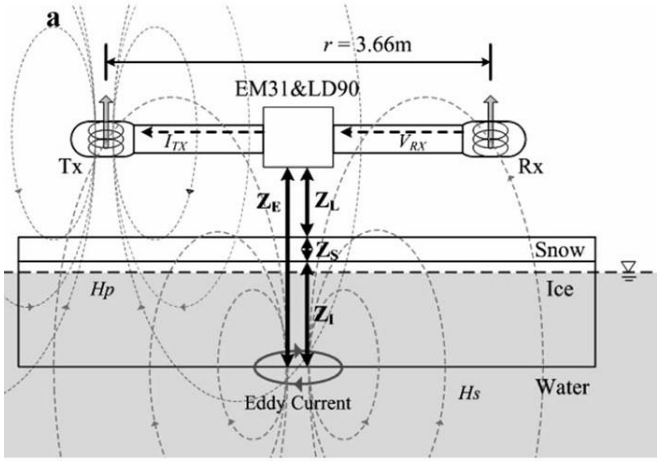

Figure 3.18 EM sounding of ice thickness [42]

When comparing the advantage and disadvantages of all the methods listed above it was concluded that the best one to peruse is the conductance/resistance measurement between the electrode plates. This was because it is cheap to implement with just basic components and should be easily scalable from the small-scale experiments to the full-scale unit.

3.5.1.3 Temperature

There are several devices capable of measuring temperature electronically each with there own benefits and draw backs. Commonly used devices have a resistance that varies with absolute temperature. These include platinum resistive thermometers (PRT), thermistors and thermocouples. Temperature is calculated with the formula below, where T is temperature, R is resistance, R_0 is resistance at 0°C and α and β are temperature coefficients of the sensor.

$$R(T) \approx R_0(1 + \alpha_T T + \beta_T T^2)$$

Platinum is used for its stability over a large temperature range (-250°C to 1000°C), PRT sensors also have an accuracy of ±0.02°C. Thermistors are made from semiconductor materials and have a temperature range of -80°C to 250°C with an accuracy of ~±0.1°C. Thermocouples use the thermoelectric effect to produce a change in electromotive force depending on temperature. The sensor chosen for this project was the thermistors as they have a large enough temperature range, can be made very small and are cheap.

3.5.1.4 Flow

There were two possible ways to measure flow in the design. The first is the use of a turbine inside the pipes that is driven by the flow of water pushing against it. This type of design could utilise a hall effect sensor that measured the rotations of a turbine in the water per minute and returned the speed of the water, or it could use the turbine to drive a generator that will generates different amounts of power depending on how fast the turbine spins. These types of measurement systems are relatively easy to make, but they may have a negative effect on the water flow so another possible system was investigated.

Ultrasound systems currently exist on the market that can detect the flow rate of a liquid in a non-contact way. They utilise sound waves and the fact that the speed of sound changes depending on what median it is traveling through to determine the speed. When there is no flow, the frequencies reflected into the pipe and back are the same. When there is a liquid present, the frequency of the reflected waves changes due to the doppler effect, the faster the movement of the liquid, the more shift seen in the frequency. With two of these positions together, one facing up stream and one facing downstream, it is possible to determine an accurate reading for the flow rate as the upstream wave will travel slower than the downstream one. These devices are very accurate and can easily handle the extreme temperature ranges that the Arctic experiences. [43]

These devices are currently available on the market for a rather large amount of money, ranging from around £200-£2000. It would be possible to design a meter that would perform the task that is required using cheaper electronics and building it from scratch, but due to the time constraints of the project, this could not be achieved.

3.5.1.5 Voltage

Measuring voltage in this project is important as almost all analogue sensors output a voltage level to be measured that is proportional to the value it is measuring. Voltage is also the only way of measuring outputs of devices as all analogue to digital converters

measure voltage levels. Therefore, all devices must output a voltage level even if measuring a value such as current.

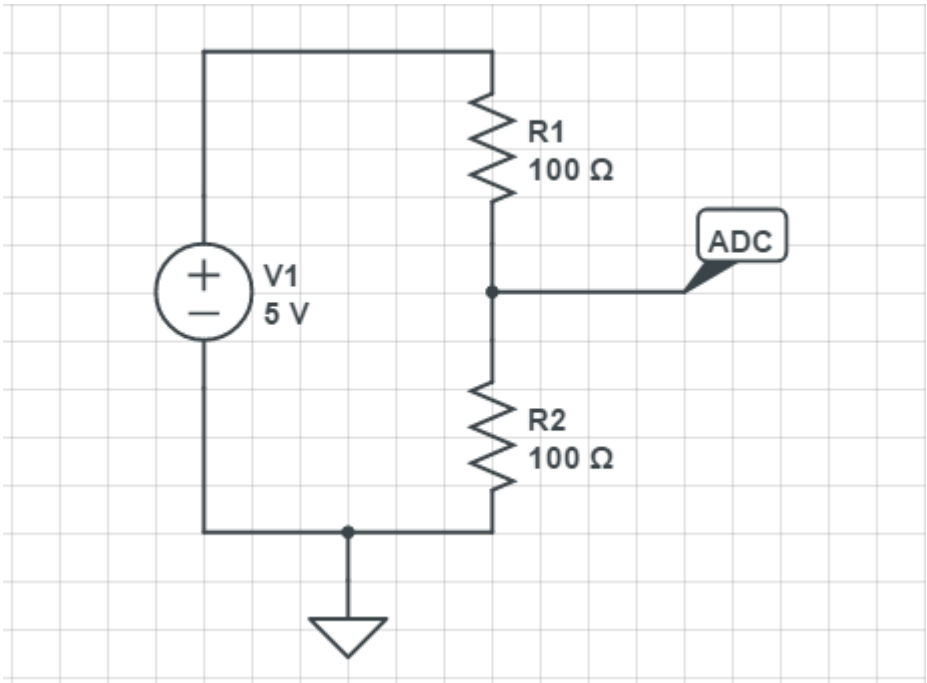

Figure 3.19 A voltage measuring circuit

Figure 3.19 shows a typical arrangement of how measuring voltages in circuits occurs. The circuit is a potential divider between R1 and R2. R2 is where the analogue sensor will usually be placed and its resistance changes depending on how whatever it measures changes. The voltage is measured where Figure 3.19 shows ADC, to calculate the voltage at ADC the following equation is used.

$$V_{ADC} = V_{in} \times \frac{R_2}{R_1 + R_2}$$

In the example given in Figure 3.19, Vin is the battery and therefore the voltage out at ADC is shown below.

$$V_{ADC} = 5V \times \frac{100\Omega}{100\Omega + 100\Omega}$$

$$V_{ADC} = 2.5V$$

An example where this is used is for temperature sensors; a temperature sensor will act as a variable resistor changing its resistance proportionally to the temperature it is measuring.

$$R \propto T$$

$$R = kT$$

In negative temperature coefficient (NTC) thermistors as the temperature rises the resistance the probe falls. Therefore, to get a reading that increases with temperature for the ADC instead of replacing R2 with the probe R1 becomes the temperature probe. This ensures as the resistance of R1 falls R2 takes a larger share of the voltage. An example is if R1 dropped to 25Ω from 100Ω the equations becomes.

$$V_{ADC} = 5V \times \frac{100\Omega}{25\Omega + 100\Omega}$$

$$V_{ADC} = 4V$$

3.5.1.6 Current

Measuring current requires turning the current value measured by the circuit into a voltage level that can be read by the ADC of the circuit. There are three main methods employed in measuring current in circuits current sense resistors, current sense transformer and hall effect sensors.

Current sense resistors, also known as current shunts convert the current of a trace into a proportional voltage that is then measured; the output voltage is small due to the size of the resistor will usually require amplification to be compatible with conventional ADCs.

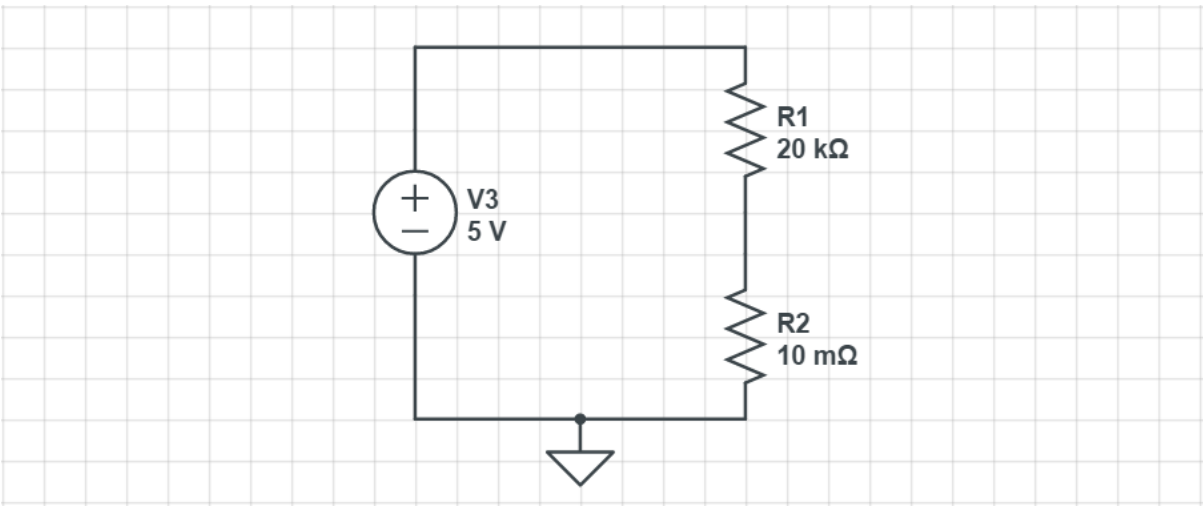

Figure 3.20 Current Sense Resistor Circuit

Figure 3.20 shows a simple circuit for low side current measurement using a current sense resistor. R1 is the load in the circuit, and this is where the current is to be measured, R2 is the current sense resistor in the circuit. Firstly, measuring the voltage across the current sense resistor gives.

$$V_{R2} = V_{in} \times \frac{R_2}{R_1 + R_2}$$

In the example in Figure 3.20 gives a voltage of.

$$V_{R2} = 5V \times \frac{0.01\Omega}{20K\Omega + 0.01\Omega} = 250\mu V$$

To calculate the current across R2 and therefore the current across the load R1.

$$I_{R1} = I_{R2}$$

$$I_{R1} = I_{R2} = \frac{V_{R2}}{R_2}$$

$$I_{R1} = I_{R2} = \frac{V_{in} \times \frac{R_2}{R_1 + R_2}}{R_2}$$

Therefore, in Figure 3.20 the current across the load, R1, is calculated as.

$$I_{R1} = \frac{5 \times \frac{0.01\Omega}{20K\Omega + 0.01\Omega}}{0.01\Omega}$$

$$I_{R1} = 250\mu A$$

When measuring low voltage equipment, current shunt resistors work well but if measuring higher voltages such as mains the lack of galvanic isolation poses a large safety risk. Furthermore, power dissipation becomes an issue when large currents are used. If measuring UK mains electricity the maximum current is 13A, putting that into the value of R2.

$$P = I^2R$$

$$P = 13^2 \times 0.01\Omega$$

$$P = 1.69W$$

Unfortunately, normal resistors are usually rated at 0.25W maximum power consumption and using that to work backwards we get a maximum resistor value of.

$$0.25W = 13^2 \times R$$

$$R \approx 1.5m\Omega$$

Therefore, using a practical value 1mΩ resistor the sense voltage generated becomes much smaller requiring a much larger amplification to convert into a useful voltage while also inducing additional noise. For lower current loads, the resistive current sense is a suitable and inexpensive option.

Hall effect sensors work on the basis that if a current carrying conductor is made into a loop, it creates a magnetic field that is proportional to the current flowing through the loop, this is then measured by a Hall effect sensor. Usually, current sense hall effect sensors are PCB mounted where one side has the loop as a track in the PCB, and the hall effect sensor is on the opposite side. Hall effect sensors have the benefit of providing galvanic isolation and therefore safe for use with large voltages and currents. Furthermore, the sensors usually come pre-packaged and therefore are resistant to elemental effects. Figure 3.21 shows a breakout board available for purchase.

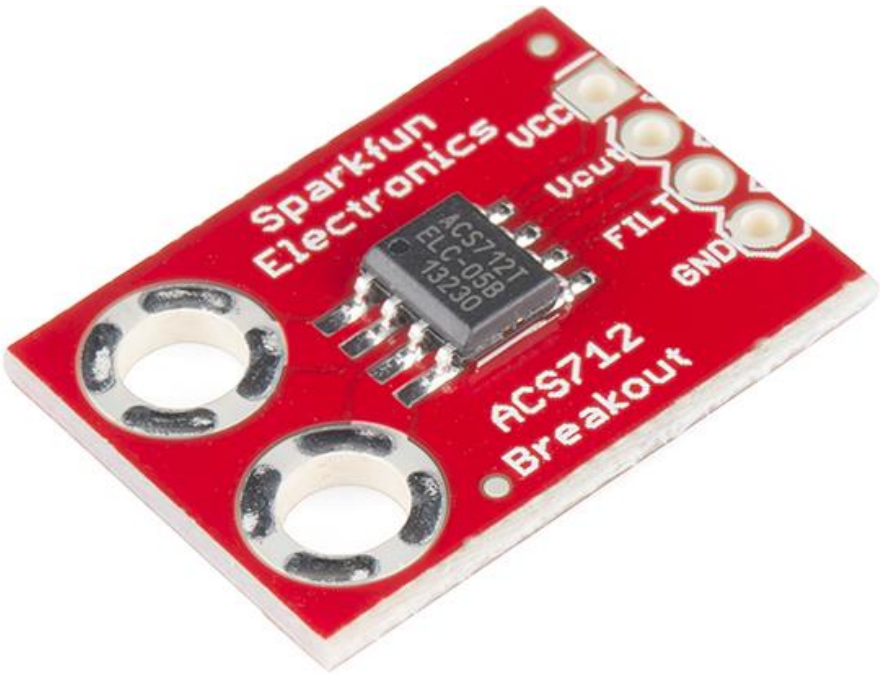

Figure 3.21 Hall Effect Current Sensor [44]

Current sense transformers work in the same way that traditional transformers do by using coils surrounding a ferrite core, current sense transformers differ in that the ratio of coils is usually vastly different. Figure 3.22 shows a current sense transformer that can be used for measuring mains electricity

Figure 3.22 SCT-013-030 Current Sense Transformer [45]

Figure 3.23 shows how the circuit works for the current sense transformer. With a 2000:1 ratio in the transformer the output is shown in Figure 3.24 generating 115mVAC from a

230VAC input. The limitation of current sense transformers is that they can only measure AC currents as the transformer requires AC voltages to work, along with the galvanic isolation makes current sense transformers the best for mains applications.

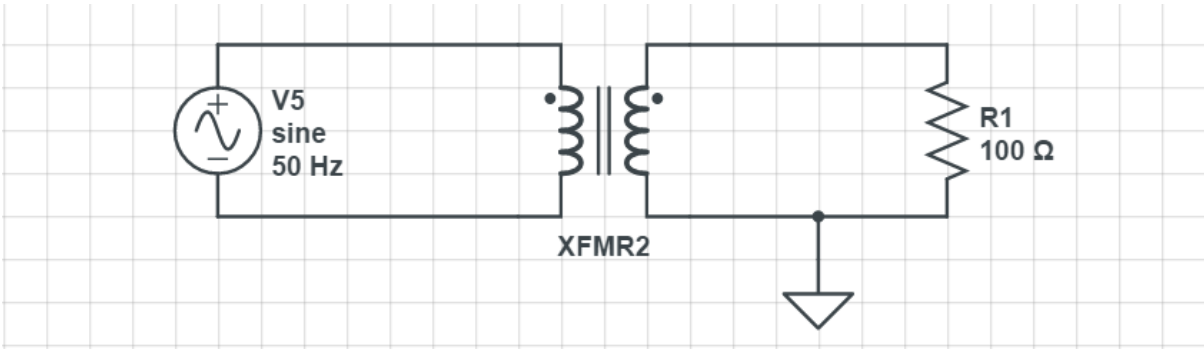

Figure 3.23 Current Sense Transformer Circuit

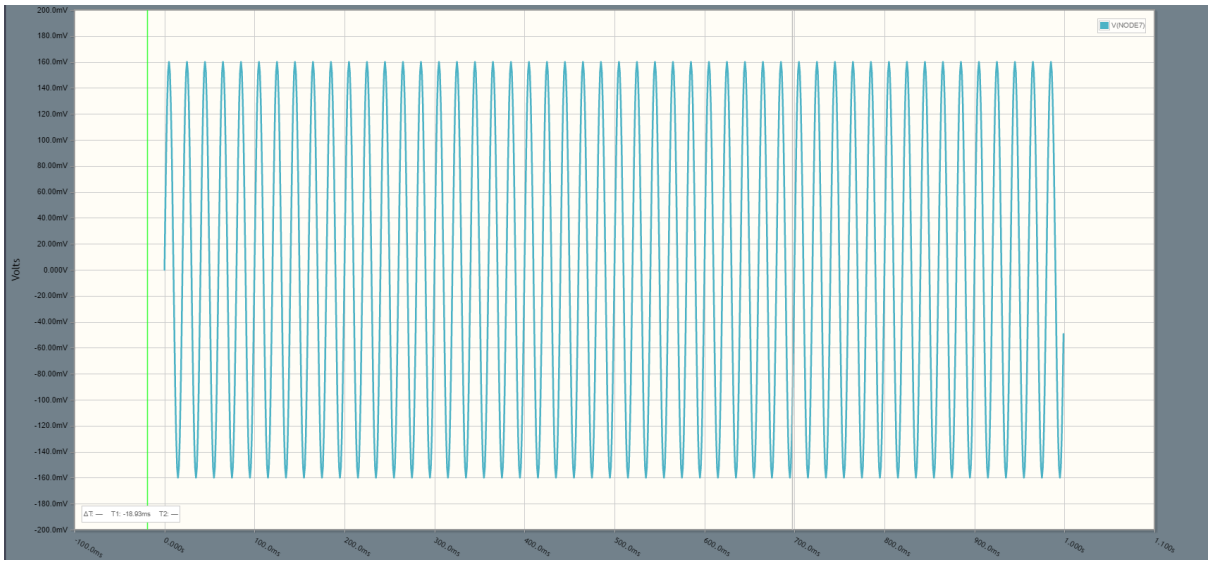

Figure 3.24 Current Sense Transformer Circuit

3.5.2 Process

3.5.2.1 ADC

An ADC or analogue to digital converter is a device that allows the conversion of discrete voltage levels created on the output of devices to be converted into digital outputs, usually in binary. ADCs are rated in bits for the available resolution and accuracy for the output of the ADC based on quantisation levels. The quantisation levels are calculated as.

$$N = 2^M$$

Where, N is the number of quantisation levels and M is the ADC resolution in bits. Therefore, an 8-bit ADC has 256 quantisation levels. ADCs have a minimum and

maximum voltage level that can be measured across and this gives the ADC voltage resolution using the equation.

$$Q = \frac{F_{FSR}}{2^M}$$

Q is the ADC voltage resolution; F is the voltage range of the ADC and M is the ADC resolution in bits. If an ADC has a voltage range of 0-5V and is an 8-bit ADC.

$$Q = \frac{5}{256} = 0.01953125V$$

When measuring inputs that have a frequency the sample rate of the ADC must be at least double the maximum frequency of the input. This is due to the Nyquist rate which determines this minimum rate. If the sampling rate is less that the Nyquist rate aliasing will occur, this is where the reconstructed signal is incorrect and information is lost.

3.5.2.2 Raspberry Pi

The Raspberry Pi created originally in 2012 by the Raspberry Pi foundation was an attempt at turning a PC into a pocketable credit card size. Priced at $35 the original Raspberry Pi offered a single core processor. Table 3.1 shows how the architecture of the Raspberry Pi has changed from a single core processor to a quad core processor while also upgrading to a 64-bit architecture. Furthermore, the clock speeds have been increased from 700MHz to 1.2GHz. Figure 3.25 shows how these improvements have affected the compute performance for each generation.

Generation	Release Date	CPU	Memory
1	May 2012	32-bit 700MHz Single Core	512 MB
1+	July 2014	32-bit 700MHz Single Core	512 MB
2	February 2015	900MHz 32-bit Quad Core	1 GB
2 ver 1.2	October 2016	900MHz 64-bit Quad Core	1 GB
3	February 2016	1.2GHz 64-bit Quad Core	1 GB

Table 3.1 Raspberry Pi Model B Versions [46]

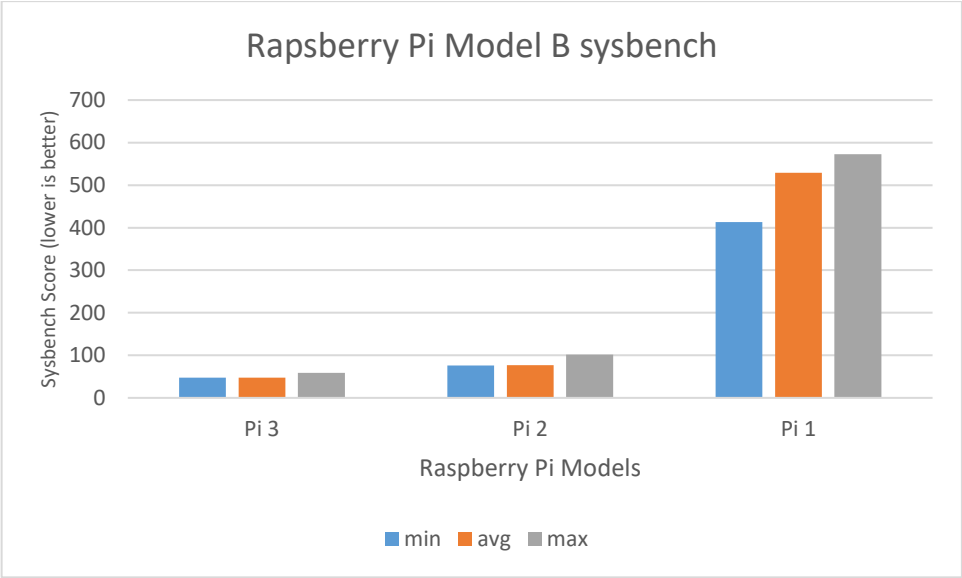

Figure 3.25 Raspberry Pi B sysbench tests [47]

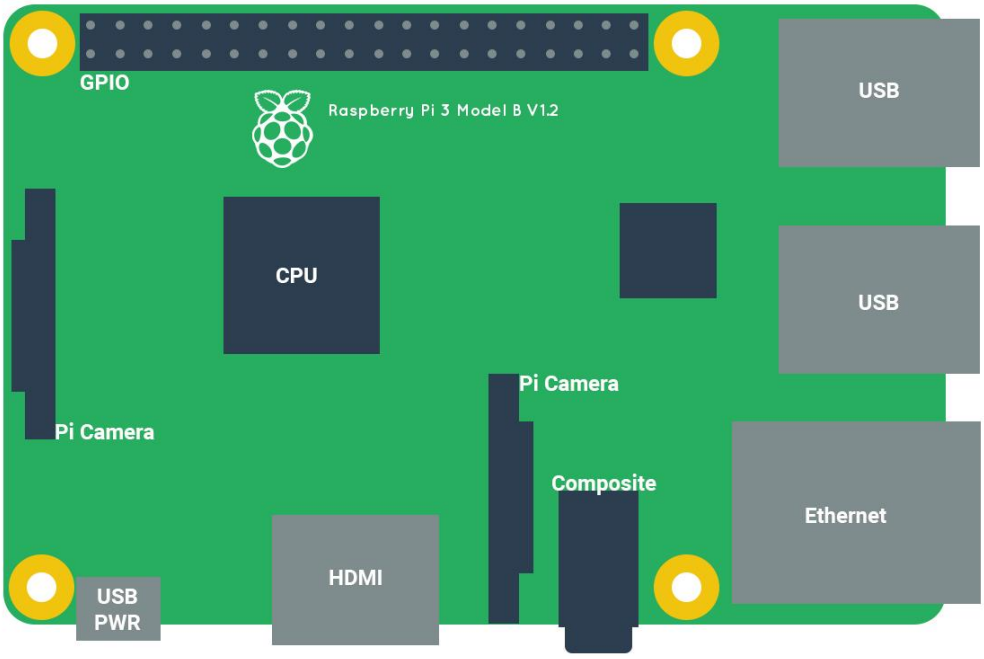

Figure 3.26 Raspberry Pi B Model 3 [46]

The Raspberry Pi allows for the merging of traditional electronics projects with a PC with networking capability running Linux through the built-in GPIO. This allows for electronics projects to start off on a breadboard and then by interfacing with the GPIO on the Raspberry Pi the project has access to the internet for internet of things projects (IoT). With the onboard processing power available it is also possible to use a vast array of sensors that require the output data to be processed before it is useful. This means that before where the processing had to be done in the cloud or somewhere similar the required

processing power is at the source. Figure 3.26 shows the layout of the Raspberry Pi B model 3; all the peripherals are situated around the outside of the board for ease of access while the GPIO are arranged as a grid of pin headers that are easy to attach wires to. During this project, the model 3 was used throughout to perform the processing and access of the data.

3.5.2.3 SPI/I2C

Communication methods between devices are important as sending and requesting data can use many input and output pins from a single device. Two common methods available for low speed electronics are SPI and I2C. I2C allows multiple master and slave devices to operate over the same communication lines whereas SPI can only have one master and many slaves. I2C is a half-duplex communication method only allowing one device to talk at a time with the other device listening. SPI differs in that it is full-duplex, allowing two-way communication. I2C has a maximum speed of 3.2Mbit/s whereas SPI does not define a maximum speed but generally it is no more than 10Mbits/s. Figure 3.27 shows SPI vs I2C when interconnecting masters and slaves. SPI requires 4 wires whereas I2C only requires two. Furthermore, the SPI master requires an additional wire per slave for the chip select pin. In this project SPI was used for interfacing between the Raspberry Pi and the ADC as that was the only available communication method on the ADC package.

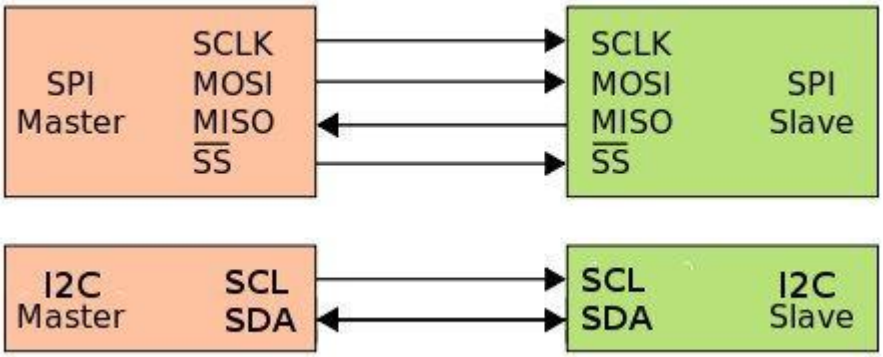

Figure 3.27 SPI vs I2C [48]

3.5.3 Outputs

3.5.3.1 Motor Control

Motor control for this project is necessary as two have been used. Firstly, the water pump that takes the water from under the ice, up through the device and out of the armature. Secondly, a motor which turns the armatures that allow the water to spread evenly around the device. Controlling these motors both on start-up and during operation must be

achieved to control the power usage of the device and the speed that the motors run. To control the motors one method used is rotor resistance control [49]. Rotor resistance control relies on a resistance that can be changed placed in series with the motor in the circuit. By changing the resistance, the maximum current flow through the circuit can be changed and therefore the speed and torque of the motor is also changed. Next, using PWM on the motor is another method where varying the available voltage by rapidly pulsing the input to the motor, this allows for fine control during operation and during start-up limiting the input rush current ubiquitous with motors.

3.5.4 Communications

Communications are an important part of this project as the devices must be able to track their progress and potential problems and relay that information back to the operator. In the Arctic there is an inherent lack of communications infrastructure for small devices and this section covers possible methods of solving that issue.

3.5.4.1 Mobile Ad-Hoc

Mobile Ad-Hoc networks are a form of decentralised networking where each node in the network becomes a router and there is no centralised administration of the network. Figure 3.28a) shows how a Mobile Ad-Hoc network might work, with all nodes in the network become a router and pass messages along through the network. This varies from a traditional network as shown in Figure 3.28b) where infrastructure exists to manage the network and devices connected to the network. In areas where it is not feasible to implement permanent infrastructure or it is remote, it is cheaper and more effective to pass messages along the chain until it can access the outside network.

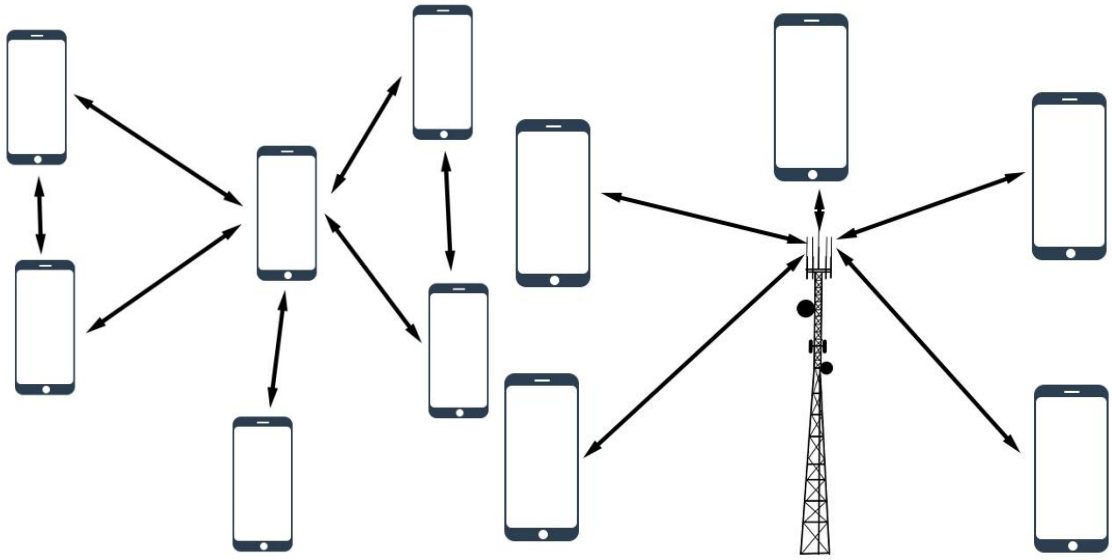

Figure 3.28 a) Mobile Ad-Hoc Network Representation b) Traditional Mobile Network Representation

Mobile Ad-Hoc networks have the advantage that they have no single point of failure; this is an advantage in remote networks as maintaining fixed infrastructure may only be possible during certain times of the year. Furthermore, Mobile Ad-Hoc networks avoid the necessity to install expensive infrastructure. This allows for more nodes, increasing resiliency and data collection. Unfortunately, due to the decentralised nature of the network, its topology becomes very dynamic, and therefore it must be able to adapt to the changes without data loss [50]. Within this project, the units must be capable of some form of communication between nodes to communicate status. There is no scope for any additional infrastructure to be installed dedicated for communication and therefore a mesh style Mobile Ad-Hoc network must be arranged.

Mobile Ad-Hoc networks have the advantage over standard mobile IP as it does not require infrastructure. Standard networks need ways of routing using DNS that require home and foreign agents. With a mobile Ad-Hoc network the lack of infrastructure allows for it to work in remote areas like disaster zones where traditional infrastructure fails. The largest problem in Mobile Ad-Hoc networks is the dynamic topology. As nodes move around the layout of the network changes, which means routing tables are also highly dynamic and must be kept up to date using dynamic routing protocols. Furthermore, links in the network may be asymmetrical, meaning that the routing information acquired for one direction cannot be used for the route in reverse, so another route must be found independently. Redundancy in the network can be high but the overall redundancy cannot

be controlled and calculating it through the routing table is computationally large. Lastly, links in the network may cause interference with each other, possibly creating a breakdown in communication. A node can also listen into nearby nodes and build a routing table based off other communications.

3.5.4.2 Data (MQTT)

Message Queue Telemetry Transport or as it is more commonly known as MQTT, is a publish/subscribe protocol designed to work on top of traditional TCP/IP and for lightweight messaging where bandwidth is limited. MQTT has clients and servers where the client publishes messages to a server, and the server is then responsible for relaying the messages to other clients that have subscribed to the feed. MQTT further adds Quality of Service (QoS) to be able to ensure that messages propagate across the network with confirmation [51]. Figure 3.29 shows how a node in a network publishes a message to the server; the server then forwards the message to the appropriate nodes that have subscribed to receive messages from the node. In this project, with the Ad-Hoc style nature of the network, the available bandwidth may be low with a high latency, meaning that MQTT is a good match to ensure that messages propagating across the network are small and are ensured delivery to the server for distribution.

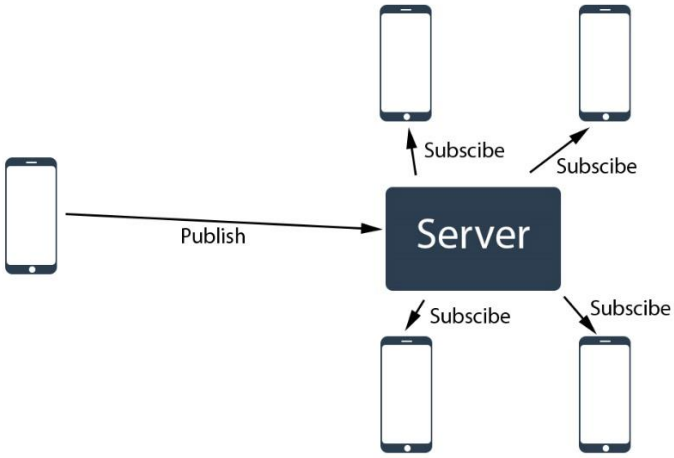

Figure 3.29 MQTT Publish/Subscribe

3.6 Business Information

The vision for the project is to have each unit costing approximately £20,000 plus finance, with the return on investment (ROI) being made in a two-year period. The aim is to sell these devices to two main groups of people. Firstly, Inuit communities would be targeted to buy the units and if needed taking a loan out to do so. Secondly, a trust consisting of a

mixed group of interested parties would also be targeted. They could be parties such as investors and Non-Governmental Organisations (NGO's) and they would involve working in the Arctic and rent them out to Inuit communities. The trust would buy many units, providing the necessary advice and knowledge to potential users.

There are several reasons why Inuit communities would be interested in getting involved with one of these units. First of all, the unit would provide a steady income for the community through the carbon credit scheme. In addition, during downtime in the summer months the units could be used as electricity generators. This would further provide the communities with an income. The pumps could also provide temporary shelters and storage facilities in remote locations across the Arctic. Finally, one other reason they would be interested is because they are helping their environment out. Helping the sea ice return to its natural level will be hugely beneficial.

On the other hand, the pumps could have a negative impact on the environment which needs to be carefully addressed. Although the units would produce no air pollution, the introduction of foreign materials could cause littering and pollution if not properly disposed of. Furthermore, any storms present in the Arctic could lead to damaged or redundant units becoming a potential hazard.

With the investors selected, the costs moving forwards were also looked at to determine their breakdown. The first cost is that of development and construction of prototypes and proof of concept models. This can be kept low by using volunteers from within the university instead of having to hire external contractors. The second is the use of site research and visits to the Arctic circle. These would be overly expensive at this early stage of development, so a contact based there was procured, with regular communication facilitated through the use of Skype virtual meetings. A similar approach is to be taken with meetings with the Inuit community. Marketing of the project will also use any volunteers or NGO's that are willing to assist with the project.

A brief description of how the project might be costed is shown in Figure 3.30 below:

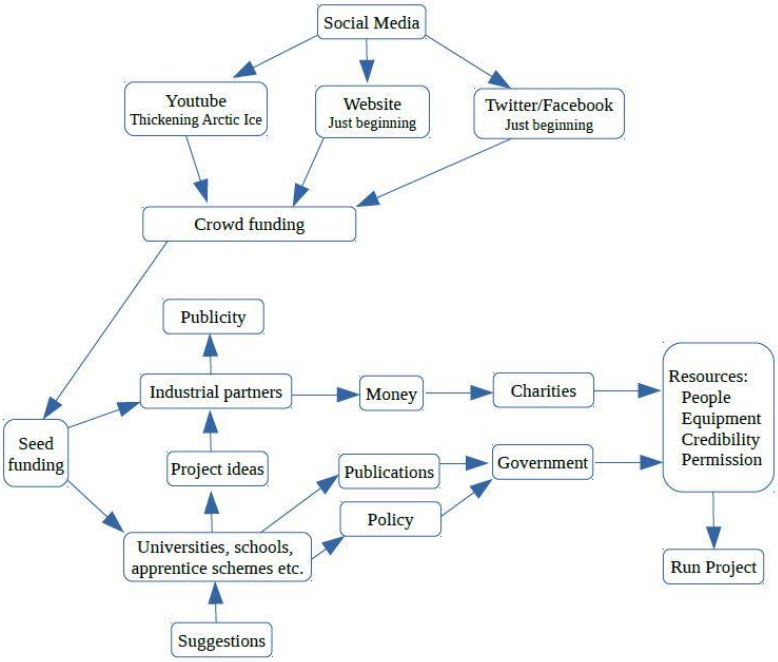

Figure 3.30 Flow diagram of funding

From the diagram, it can be seen that the first step to raising money would be to use social media to generate buzz around the project. With the project being discovered by more of the public, a crowd funding platform such as Indiegogo or Kickstarter could be used to pull in funds from those interested, with incentives being offered depending on how much money is offered towards the project. With this initial funding, it would then be possible to partner with corporations or investors to finance the project. These investors or corporations may not be willing to directly finance the project, but it could be possible for them to make contributions to a charity that it is partnered with, possibly leading to positive publicity for the contributors and for the project, which may lead to increased funding. Educational institutes would also be targeted in a similar manor as a place where project ideas could be developed and improved, without the need to invest much capitol. These involvements would also further the outreach of the project, with papers and publications being produced that can be distributed to the science community. With these papers giving good credibility to the project, governments could then be approached who might offer more resources in the form of permissions, equipment or people.

The business model that is proposed to be used is very similar to that of the one taxi businesses utilise. In this case, an ‘Arctic Showroom and Workshop’ would work as a franchise for spare parts and maintenance of the system, acting as mediatory between the supplier and the Inuit Company. This company would consist of teams of two or more Inuit’s who bought the system from the company that produced them based in Wales. The Gold Standard or a similar company would regulate the operation of the system to ensure that the ice was being thickened sufficiently, allowing the Inuit Company to generate income by selling Carbon Credits using Gold Standard.

Chapter 4: Design and Methodology

4.1 Design

4.1.1 Design 1

The initial design was created to test whether the theoretical design we had of using a helicopter hose that pumped water up, and through its spinning action, distributed it out through 3 plastic tubes was feasible. With the Rule 4000 being the pump that was most suited for the flow rate that was required, this was used as the main pump to get the water through the pipes. A view of the initial design is shown in Figure 4.1 below.

Figure 4.1 The Initial design

This design featured three distinctive elements which differed from further designs. Due to the way the pump is made, it featured a U-bend to attach the pump to the main stem. The initial thinking behind this was that for the pump to be working in its most efficient manner, it should be acting in the way that it was designed to act, which is face up as shown in Figure 4.2 below.

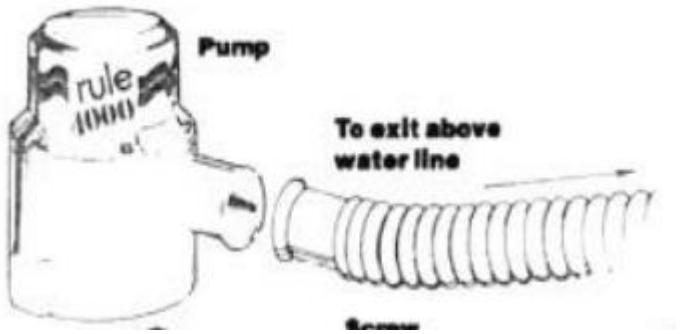

Figure 4.2 Diagram of how the pump should be positioned. [52]

With the pump connected to the main stem, the next thing that was present in the design was the height of the stem. Due to the desire to achieve maximum distance from the device, it was theorised that the maximum initial height that could be achieved would greatly help increase the distance. This is due to the SUVAT mechanics equations where the higher up an object's initial start is, the longer it will take to hit the ground and therefore the further it will travel horizontally.

Another aspect of the design that was implemented was gearing and a drive chain to allow the device to spin. The initial gearing of the design was set to be 1:1, with the motor aiming to spin at 2700rpm and therefore trying to spin the entire design at that same speed. This was implemented due to the theory that the higher the speed that the device spins, the higher the exit velocity and therefore the further the water will travel, again due to the same SUVAT equations that were used to determine the height of the stem.

4.1.2 Design 2

This design was done to improve on results that were found from the first design. For this design, the key change was that the pump changed position. Instead of the pump being directly upright, it was changed to be on its side, and the pumps exit now pointed upwards. This was done to remove the U-bend that was implemented into the first design which once removed would allow the water to flow upwards with less resistance.

A U-bend in a pipe causes a loss in pressure and velocity of the moving water so limiting this would be advantageous. These pressure losses are caused by friction and momentum exchanges which come as a result of the water flowing in a different direction, which causes fluid separation from the inner wall. The bends cause fluid to move to the outer

side of the pipe. It then comes back towards the inner side, and this creates a double spiral flow of water which is shown in Figure 4.3.

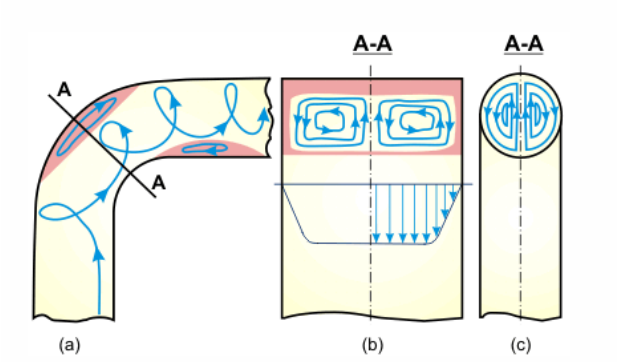

Figure 4.3 shows the double spiral flow of water that is caused by a bend in a pipe a) longitudinal section, b) rectangular cross-section and c) circular cross-section [53]

The amount of pressure that is dropped is determined by the bend loss. The larger the angle, the larger the loss, which is shown in Figure 4.4. The radius of the bend in the pipe also has an impact on the losses as well as the loss coefficient. Removing the U-bend reduces this loss.

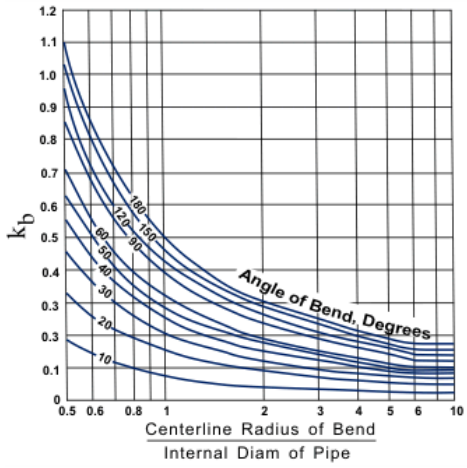

Figure 4.4 shows a graph of the loss of different angled bends, showing the loss coefficient against the size of the pipe (Babcock & Wilcox Co, 1978) [53]

In addition, a shorter head was used for this design. This was also done to limit the drop in pressure that the water might experience, to maximise the distance at which the water could be distributed. Also, from the data sheet of the pump we used, it is shown that increasing the vertical distance the water needs to be pumped dramatically reduces the output flow. A shorter head was used because of this reason.

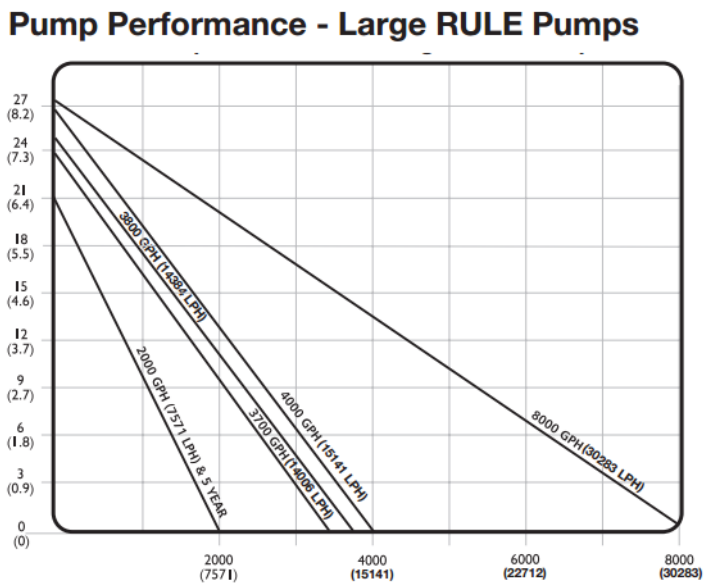

Figure 4.5 shows a graph of the maximum output flow against the height of the head for the pump used in experiments.

The pump used had a maximum output flow of 15141 LPH. For design 1 the height of the apparatus was at 1.8m. This meant the maximum output flow was limited to approximately 11750 LPH, which meant it was only working at 77.6% efficiency. [37] To improve this, a shorter head was used so the output flow could be increased. For this design, the apparatus was changed to a height of 1.1m. This now meant the optimum output flow was increased to approximately 13060 LPH and the efficiency of the pump was now in theory at 86.3% of maximum output.

Also, in this design, the gearing ratio was changed. An 8:1 gearing ratio was implemented to try and optimise the effect of spinning the device and increasing the distance at which the water could be distributed. The first design used a 1:1 gearing ratio which isn't enough. The motor wants to spin at a rate of 2700RPM, and with a torque of only 0.35Nm. It is not possible to achieve this spin rate. Therefore, it was changed to a ratio of 8:1, reducing the spin to roughly 340RPM but increasing the torque to 2.8Nm.

4.1.3 Final Design

Further changes to the design were made based on the results of the experiments of the previous designs. The major change made was to reduce the spin rate further so as not to use the absence of centripetal force in the rotary system, to increase the distance travelled by the water. Instead, the aim was to use most of the power provided for the pump, and only a minimal amount to rotate the nozzles, allowing the water to be distributed evenly

across the ice. The motor to be used in this case is 7W and has a built-in gear ratio of 50:1 to give it a low RPM and high torque. The 8:1 pulley can also be used to increase the torque further, ensuring the motor can spin at peak efficiency.

Another change to be made was to put a laminar flow nozzle on the outlets to further the distance travelled by the water in the air. With the previous design, the high spin speed of the stem meant the water leaving the nozzle quickly broke apart and became many water droplets. Many water droplets have a greater surface area than a single stream of water of the same volume, so the droplets are affected more by air resistance. This means for a given flow rate of water in the air, liquid in a laminar flow would travel the furthest.

4.1.4 Instrumentation

4.1.4.1 Ice Thickness

From the research of possible methods to measure ice thickness, the chosen one was to use two parallel plates with several electrodes across them and measure the conductance or resistance between them. The top-level design of the circuit is shown below; the sensor plates are placed in the water with them connected to the interface circuit. The circuit reads the resistance or conductance and produces a DC voltage level that is read by an analogue to digital converter (ADC). This feeds onto the microprocessor where the readings between each electrode are processed to produce a value for the ice thickness.

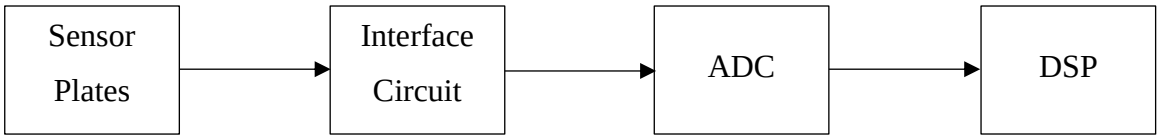

Figure 4.6 Top level design

For this method, it uses two identical plates with several electrodes across them. This could be made with a printed circuit board, but the chosen way was to use a piece of stripboard as it is cheap and already in the required layout. The standard size for strip board is to have a spacing of 2.54mm; this would limit the resolution of the sensor but by taking readings between all the electrodes of each plate rather than just the opposite ones, the resolution should go below 2.54mm. For the small-scale experiments, the ice thickness will be in the range of 0mm to 20mm therefor 12 electrodes per plate was chosen. This gives a range of up to roughly 30mm of ice thickness measurement.

There were several iterations of the interface circuit due to problems with it that arose when being tested. There were, however, parts of the circuit that worked fine and did not need to change these are as follows.

Careful consideration of how to power the circuit is important as there is current flowing through water being tested. Because of this, it must be isolated from mains power. This was done by just using a battery to power it. As is mentioned further on, the multiplexers and op amps can both be powered by 12V, so a single 12V lead acid battery will suffice. Lead acid batteries do not supply a steady 12V level, so a buck-boost converter was used to keep it at the required 12V as the battery level changed. The ADC chosen requires a 5V supply so to produce that from the 12V supply an LM7805 voltage regulator was used to produce 5V.

As the interface circuit is to be battery power and the Raspberry Pi is powered by a mains power supply, there needed to be some form of isolation between them. To isolate the multiplexers from the Pi optoisolators were used. The chosen devices were KB817, where Figure 4.7 shows the operation of them. The input is connected to a Raspberry Pi GPIO pin, and VCC is connected to the battery, with the output going to one of the address pins on the multiplexer. When the input is high, the output becomes shorted to ground, so the control becomes inverted. As the GPIO pins are controlled in software, the inversion is no issue.

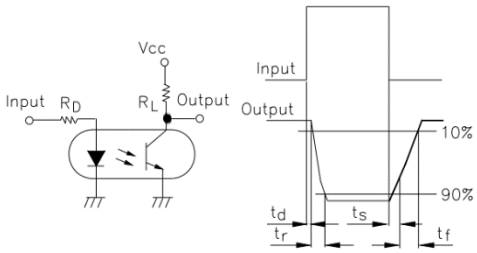

Figure 4.7 Opto-Isolator Operation [54]

On each sensor plate, there are 12 electrodes, and each of these must be separately connected to the interface circuit. This can be done by multiplexing the connections. After researching different multiplexers, the chosen one was a DG406. This is an analogue multiplexer, so it also acts as a demultiplexer. Therefore, the same one can be used on the input and output plate. It can be powered from a single 12V supply and has 16 channels

that would allow for expansion of the sensor plates. To control it there are 4 address pins that are opt-isolated from the Raspberry Pi.

For the digital signal processing to be done an ADC is required, as the Raspberry Pi has no analogue inputs. The one used is an MCP3008, it has a serial peripheral interface (SPI) bus to allow it to communicate with the Raspberry Pi. It is powered with 5V and has a 10-bit resolution that is more than adequate to provide a clear reading from the interface circuit. It has a max sample rate of 200KHz which is far more than needed as water does not freeze very fast at just below 0°C.

To do the digital signal processing, a Raspberry Pi was used as it has both an SPI and I2C interface to connect to the ADC. It also has several GPIO pins that can be used to easily control the multiplexers. The operation of this and the DSP can be found in section 4.2.1.

Figure 4.8 shows the full circuit that was constant throughout the different iterations of the interface circuit. The Pi controls the connection of the electrodes to the interface circuit through the multiplexer. The Interface circuit feeds into the ADC which is connected to the Pi where the readings are stored, and the digital signal processing is done.

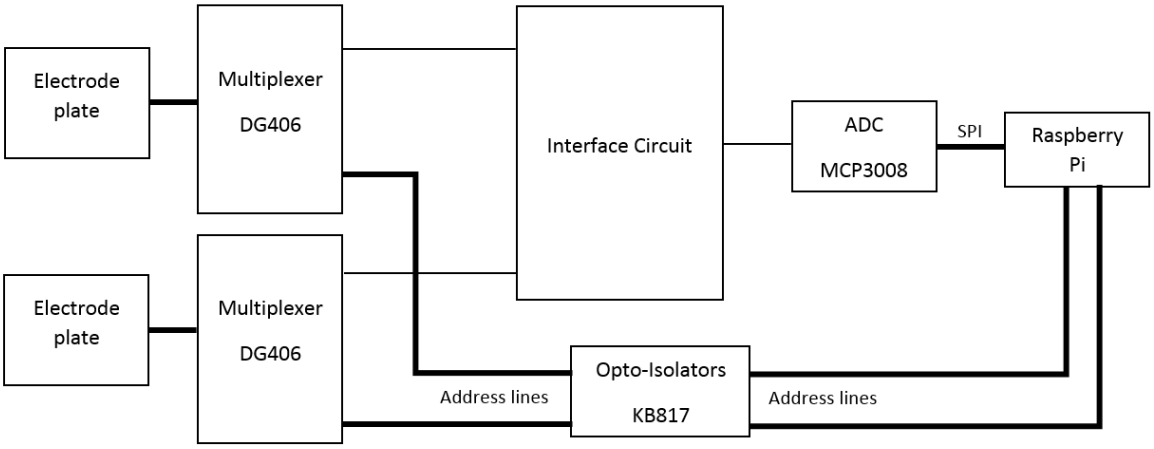

Figure 4.8 Ice thickness measurement circuit

The setup used for testing is showed in Figure 4.9. A clear tub of water was put in a freezer with the sensor placed with the top above the water level; this was important as both the top and bottom level of the ice must be known to calculate its thickness. All sides apart from the top of the tub were insulated with a towel to ensure the ice froze from the

top down. A camera was used to visually monitor the ice level for calibration. A ruler and LED's above and behind the ice were used to aid the calibration.

Figure 4.9 Ice thickness experiment setup

Each experiment was done over roughly 20 hours to allow ice thickness to increase enough to cover the whole of the submerged part of the sensor. Readings of the conductance were taken between each of the 12 electrodes on one plate and the 12 electrodes on the other plate to give 144 readings. For each of the 144 readings, 100 samples were taken over 1 second and the average of that stored. This meant that every time a reading was taken it took 144 seconds. The readings were then taken at 2-minute intervals across the entire experiment time.

The first design was to measure the resistance of the water between the plates. This was achieved by passing a voltage across a potential divider and reading the output. The sensors were multiplexed on the low side of the divider. Figure 4.10 illustrates the circuit. R1 was also multiplexed with different values of 47KΩ, 200KΩ, 1MΩ and 70MΩ to find a suitable value for the circuit. Trial and error was used as calculating the expected resistance of the water/ice between the electrodes would be difficult due to the dimensions being unusual.

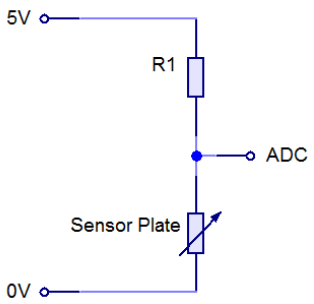

Figure 4.10 Potential divider

This design was unable to represent the change between water and ice as is shown in Figure 4.11. The graphs show the how the resistance between each parallel electrode changes with time as the water freezes. Graph (b) shows only the results between the two centre electrodes, the resistor used for R1, in this case, was the 47KΩ. The data shows that the values were being clipped long before the ice was forming, meaning that the resistance is over 10MΩ when the ice was formed. Increasing the value of R1 only made the data more sporadic where no useful conclusions could be made from it.

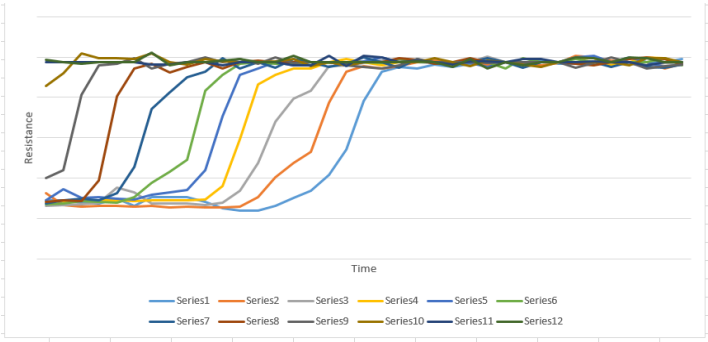

(a)

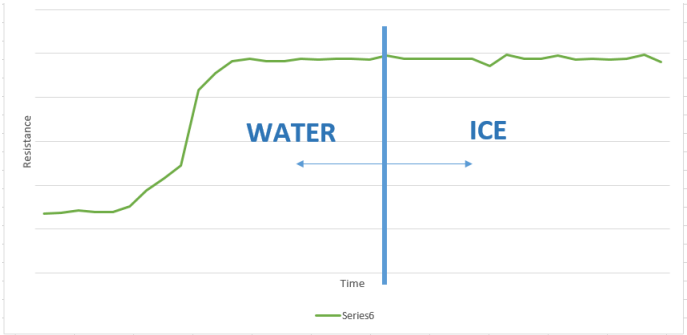

(b)

Figure 4.11 Potential divider design results, full data set for series 1 the bottom electrodes to series 12 the top electrodes (a) just the data for the middle electrodes (b)

Due to repeat issues with the measurement of resistance, the second design changed to work with the conductance instead. It was a similar design to the previous one, but instead of a DC supply, AC was used instead. Also, instead of a potential divider, a Wheatstone bridge was used to give a much higher level of precision. The output was then amplified and half-wave rectified with a single diode to produce a DC voltage level that changed with the conductance.

For this circuit, an AC signal was required. Figure 4.12 shows the circuit used to generate the signal. R1 and C2 form the RC network of the circuit to provide a square wave with a frequency of roughly 7.2 kHz. L1 and C3 form an LC circuit with a resonant frequency of 7.2KHz to turn the square wave output to a sine wave. C4 then removes any DC from the signal; this then feeds into the Wheatstone bridge.

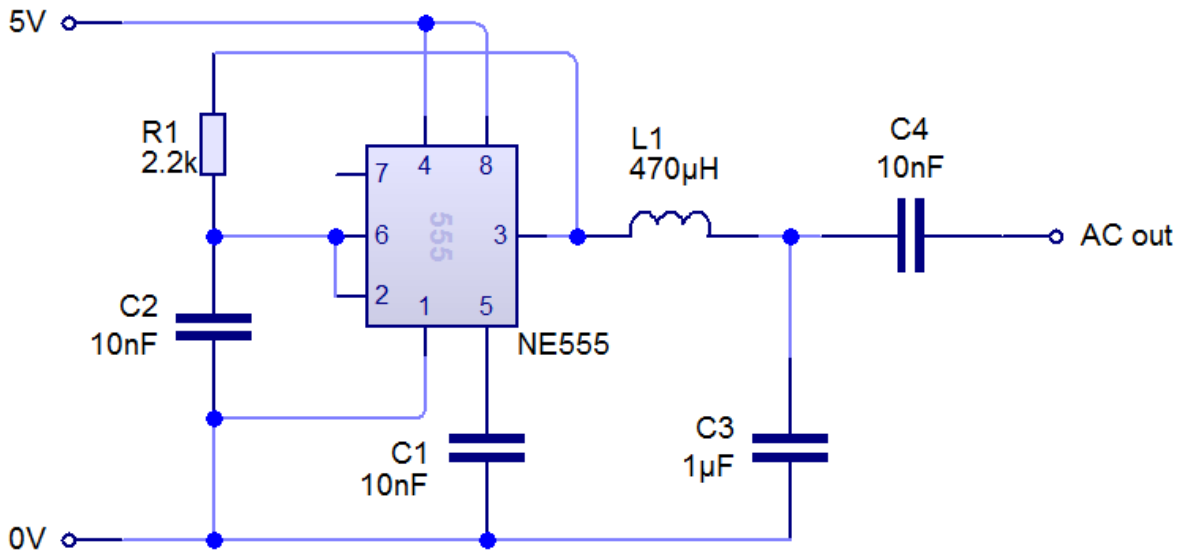

Figure 4.12 Sine wave generation circuit

To amplify the signal across the Wheatstone bridge, an instrument amplifier was used (AD623). This had to be used over a standard op-amp as a high impedance input was required. It also has a high common-mode rejection ratio, so there is little noise on the signal once amplified. The gain is set with the value of resistor R_G that is between pin 1 and 8 of the op-amp, for this circuit a 10K potentiometer was used so it could be easily adjusted to a suitable level.

As the water cooled and eventually formed into ice, the amplitude of the output sine wave changed. There was also a phase change between the input and output sine wave, but this was a very slight change and would have been difficult to measure accurately. The output

of the op-amp was then rectified with a single diode and smoothed with a capacitor. This meant for an easier reading of the amplitude change and less work for the DSP to do.

With the new design, the change from water to ice could be quantified from the interface circuit. The values read by the ADC are arbitrary as it could not give an accurate value of the conductance due to the tolerances of the components. This means that for the circuit to give a result of ice thickness from the data it collects it has had to be calibrated, the process of which is described in section 4.2.1.

4.1.4.2 Power

Calculating power in circuits is achieved by measuring the voltage and current within a circuit and using the equation.

$$P = VI$$

In this project monitoring the power draw is important so a power budget can be decided and monitored during testing. Furthermore, in the final version monitoring the power usage is important as it can be used to control and make decisions based on input power and available power. Additionally, monitoring the voltage of the battery infers its charge level based on Table 3.1 shown below.

Percent (%)	Voltage (V)
100	25.46
90	25.24
80	25
70	24.74
60	24.48
50	24.2
40	23.92
30	23.62
20	23.32
10	23.02

Table 4.1 24V Battery Charge Levels

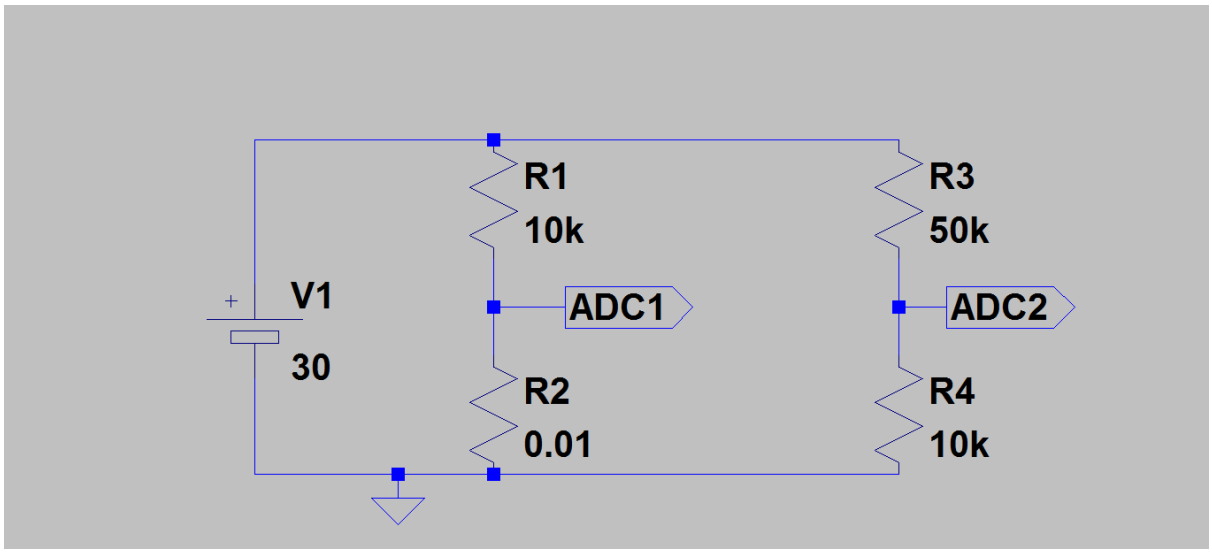

Figure 4.13 Power Monitoring Circuit

The circuit shown in Figure 4.13 is the basis of the power monitoring circuit. It is made up of two parts, a voltage divider and a current shunt.

The maximum voltage of the battery is around 26V, therefore for a round number the maximum voltage will be assumed to be 30V. The ADC requires a maximum input voltage of 5V and to achieve this the following value for R3 and R4 is used.

$$30V = 25V + 5V$$

$$R3: R4 = 25: 5 = 50K: 10K$$

This ensures a max value of 5V on the ADC input. To calculate percentage value of the battery first the equation of the line for the battery values is calculated.

$$y = 0.8564x^3 - 59.844x^2 + 1427.2x - 11578$$

This gives the percentage value when measuring the voltage across the battery. This circuit gives a proportional value so a separate equation must be calculated to adjust for this.

$$y = 184.98x^3 - 2154.4x^2 + 8563.2x - 11578$$

This equation will take the input voltage for the ADC and convert it into a percentage value of the battery.

Finally, calculating the voltage of the battery for the power equation is calculated as.

$$V_{Battery} = \frac{V_{ADC} \times (R1 + R2)}{R2}$$

For the current measuring part of the circuit, R1 acts as the load on the battery and therefore the current needs to be measured through the same trace. Therefore, R2 is the current shunt; it is a 10mΩ resistor with a maximum power dissipation of 5W. With the maximum power dissipation value given in the datasheet, the maximum current draw through the resistor is equated.

$$P = I^2 R$$

$$I = \sqrt{\frac{P}{R}}$$

$$I = \sqrt{\frac{5}{0.01}} = 22.4A$$

With a battery voltage of 24V, the maximum power draw of the load resistor R1 is calculated as.

$$P = VI = 24 \times 22.4 = 537.6W$$

This is the maximum power draw the circuit can have without taking the current sense resistor above the specification. If the project requires more power, then a new current sense resistor must be specified.

To measure power firstly, the voltage of the battery was calculated as.

$$V_{ADC2} = V_{Battery} \times \frac{R4}{R3 + R4}$$

$$V_{Battery} = V_{ADC2} \times \frac{(R3 + R4)}{R4}$$

$$V_{Battery} = V_{ADC2} \times 6 = 6V_{ADC2}$$

Secondly, where R1 is the load on the circuit and R2 is the shunt, current through the load was calculated as.

$$I_{R1} = I_{R2} = \frac{V_{Battery} \times \frac{R_2}{R_1 + R_2}}{R_2}$$

Therefore, the power draw in the circuit is calculated as.

$$P = IV$$

$$P = \frac{V_{Battery} \times \frac{R_2}{R_1 + R_2}}{R_2} \times 6V_{ADC2}$$

$$P = \frac{V_{ADC1} \times V_{Battery}}{R_2}$$

$$P = \frac{V_{ADC1} \times 6V_{ADC2}}{0.01}$$

This final equation gives the value of power through the load in the circuit in watts and once converted into its code equivalent taking into consideration the resolution of the ADC. This is how power was monitored in this project.

4.1.4.3 Temperature

After looking at the possible methods for measuring temperature the chosen way was to use a thermistor. As an ADC is already being used for the ice thickness measurement, another analogue measurement can easily be added.

The essential properties of the thermistor are that it is waterproof and can go to sub-zero temperatures. The thermistor chosen was an NTCAIMME3C90373, it is an NTC thermistor meaning it has a negative temperature coefficient. It has a temperature range of -25°C to +105°C, an acceptable temperature range for the small-scale experiments but in the Arctic, temperatures can go down to -40°C. For use in the Arctic the thermistor can be changed to a more suitable one, although the circuit would not need to change, just be recalibrated. The resistance of the thermistor ranges from 580Ω at 105°C to 130KΩ at -25°C but the temperatures in the small-scale experiment should not exceed room temperature. Therefore, the circuit only needs to measure down to 10KΩ at 25°C.

For measuring the resistance of the thermistor accurately, a Wheatstone bridge circuit was used.

Figure 4.14 shows the setup of this circuit where VR1 represents the thermistor. The chosen values of the resistors are such that Vout ranges from 0V to 2.5V as the temperature changes from +25°C to -25°C.

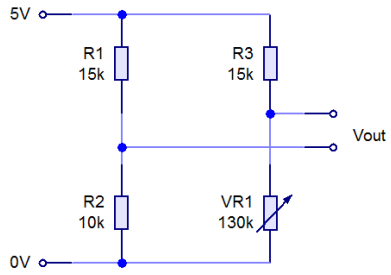

Figure 4.14 Wheatstone Bridge circuit

The ADC used is an MCP3008 that has a 10-bit resolution with an input voltage range of 0V to 5V. To utilise the full potential of the ADC an amplifier with a gain of 2 was used to interface the Wheatstone bridge to the ADC. An AD623 was used as it is an instrument amplifier and therefore has a high input impedance that is required for this use. The gain is set by changing the value of resistor RG, for a gain of 2 a 100kΩ resistor was used. The full circuit is shown in Figure 4.15, where Rt is the thermistor. To take readings at several points across the system Rt can be multiplexed with several thermistors similar to how the ice thickness electrodes were used. This means that extra op amps are not required thus reducing the size and cost of the circuit.

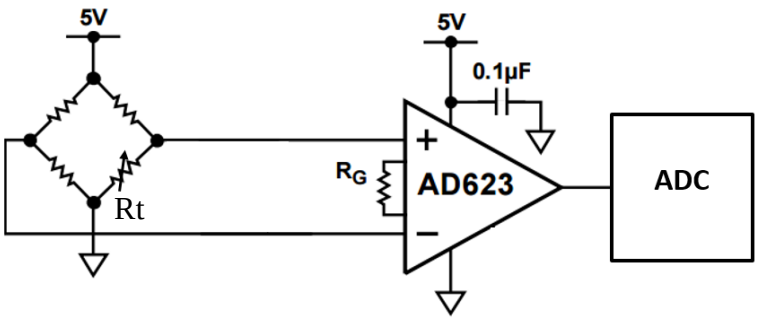

Figure 4.15 Temperature Sensing Circuit [55]

4.2 Methodology

4.2.1 Instrumentation and Calibration

As there is a tolerance in the components used for the temperature measurement circuit the reading given is most likely to be wrong. For this reason, the device must be calibrated before it can be used. The calibration is done by placing the sensor in a varied set of temperatures with a thermometer that is known to be calibrated. Once the readings have been done the difference can be adjusted so that it matches the thermometer. The adjustments are done with either hardware or in the software.

The calibration experiment was done with a food grade digital temperature sensor which has a temperature range of -50°C to 300°C with an accuracy of ±0.1°C. The thermistor was placed with the end in a beaker and the thermometer next to it. Boiling water was poured in to cover both sensors and a reading was taken. The beaker was then left on a table at room temperature with readings taken for every 5°C change in temperature. The data in Table 4.2 shows how the readings vary over the course of the experiment.

Digital Thermometer (°C)	Thermistor (°C)	Percentage difference
100	99.6	0.0004
95	94.7	0.0003
90	89.6	0.0004
85	84.6	0.0004
80	79.8	0.0002
75	74.7	0.0003
70	69.6	0.0004
65	64.6	0.0004
60	59.7	0.0003
55	54.6	0.0004
50	49.6	0.0004
45	44.8	0.0002
40	39.7	0.0003
35	34.7	0.0003
30	29.7	0.0003
25	24.6	0.0004
20	19.7	0.0003

Table 4.2 Temperature experiment data

The data shows that the difference in temperature readings is only very slight but most importantly the difference is almost the same across the experiment range. This meant that the calibration could be done easily with hardware by changing R2 in the Wheatstone bridge with a 10K potentiometer. The experiment was repeated, but with the

potentiometer in place, it was then adjusted so that the thermistor readings matched the digital thermometer.

The interface circuit was connected to the ADC as is shown in section 3.5.1.3, the ADC connects to the Raspberry Pi and gives a reading of voltage. To convert the reading of voltage to temperature, the value is first divided by the gain of the amplifier. Resistance is then calculated with the potential divider equation to give a value of resistance for just the thermistor. From the resistance value the temperature can be calculated with the equation below. Where T is temperature in kelvin, R_{25} is the resistance of the thermistor at 25°C and A, B and C are known constants for the thermistor.

$$\frac{1}{T} = A_1 + B_1 \ln\left(\frac{R}{R_{25}}\right) + C_1 \, ln^2 \left(\frac{R}{R_{25}}\right) + D_1 ln^3 \left(\frac{R}{R_{25}}\right)$$

The design of the ice thickness measurement circuit allows it to differentiate between water, ice and air. As there are 12 electrodes on both sensor plates and a reading is taken between each of them there are 144 values given each time a measurement for ice thickness is taken. Each of the 144 values are between 0 and 1024 as a 10-bit ADC was used. These values needed to be reduced to one number for the ice thickness in mm. The calibration experiment was outlined in section 4.1.4.1 with readings taken at 2 minute intervals. The camera in the freezer took a photo each time a reading was taken so the actual ice thickness was known. Figure 4.16 shows one of the pictures taken half way through the experiment, looking at the side of the water tub. In the picture the red line is at the bottom of the ice with the blue line at the top of the ice.

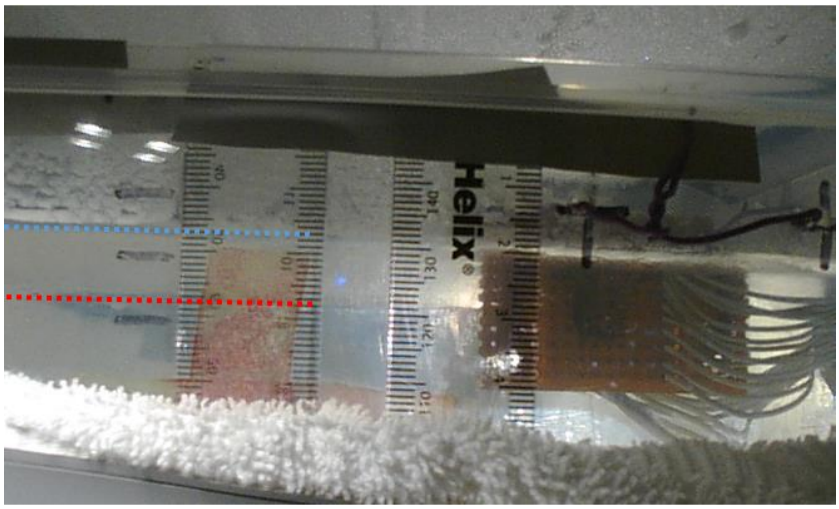

Figure 4.16 Ice thickness calibration experiment photograph

Each photo taken during the experiment was analysed to produce a data set for the ice thickness to the nearest mm over time. This data set was used to cross reference the data taken for the arbitrary conductance of the ice/water between the plates. Figure 4.17 represents the values taken between only the parallel electrodes. The numbers on the y axis are just the output voltage of the interface circuit but they do represent conductance.

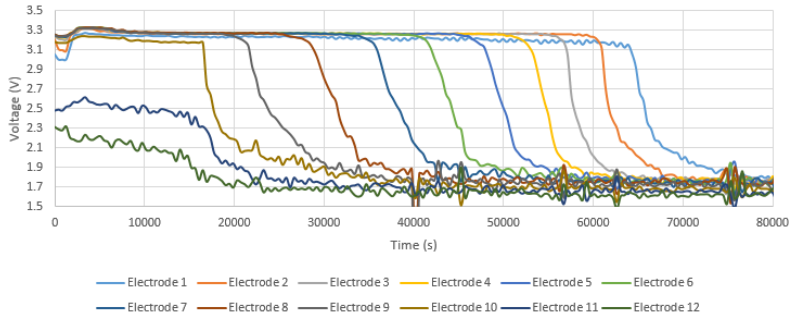

(a)

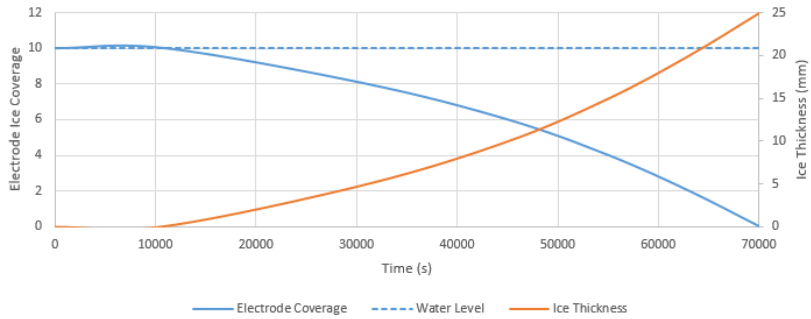

(b)

Figure 4.17 Ice thickness experiment data (a) raw values and (b) ice thickness/coverage

Looking at the graph electrode 1 is the bottom parallel electrodes and it is known that electrodes 11 and 12 are above the water level. When this data was compared with the ice thickness graph it shows that the voltage drops from roughly 3.3V once the ice forms over the electrodes. However, the electrodes above the water stay at about 2.3V until ice begins to form beneath. This means that the Pi must store the readings for it to calculate ice thickness. To do this with only the data from the parallel electrodes the processing done was to set a threshold at roughly 3.1V, below which ice has formed. More complex processing was done to find the top of the ice. For the submerged electrodes, the voltage level transitioned from 3.3V to 1.7V in a short period, the voltage level for the electrodes above the ice slowly falls from 2.3V. The Pi looked for this pattern to find the top of the ice. From this processing, the electrodes at the surface of the ice were known as well at

the ones at the bottom of this ice. Since the electrodes are also known to be 2.5mm apart, the ice thickness could be calculated with a resolution of 2.5mm. Further more complex processing must be done with the 144 values from the full data set of each reading to increase the resolution below 2.5mm. This was unable to be done in the time frame given due to the long delays in designing and testing the interface circuit.

Results and Discussion

5.1 Lake Experiments

5.1.1 Experiment 1

5.1.1.1 Water Range

This experiment was done to see how far the water travels from nozzle to ground with a changing nozzle diameter. Design 1, explained in section 4.1.1 was used for this experiment.

Distance Travelled (m)	Nozzle Diameter (mm)
2.9	10
3.2	17
1.9	20
1.5	25
0.7	35
0.6	40

Table 5.1 shows a table of results for the water range experiment

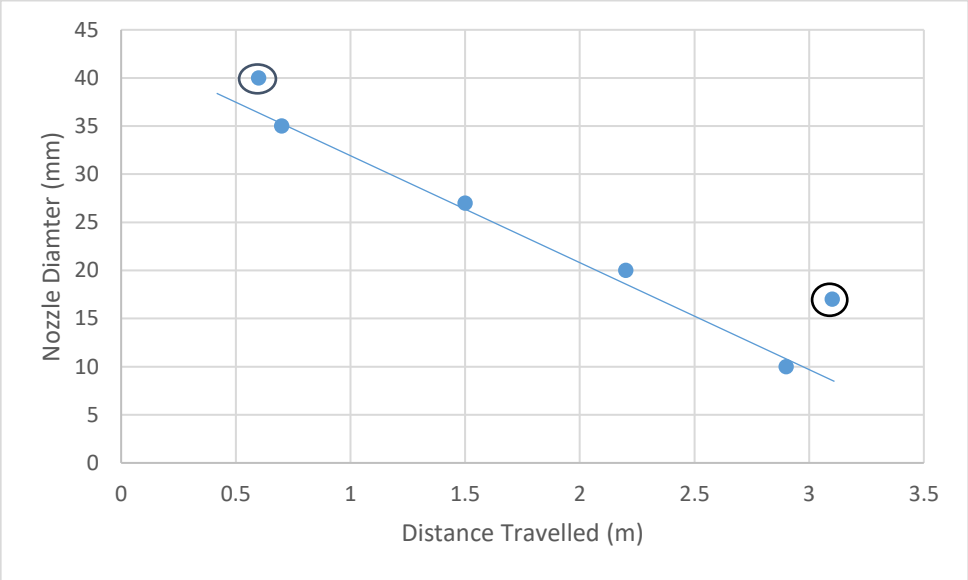

Figure 5.1 A graph showing the relationship between the nozzle diameter and the distance the water travelled from the end of the nozzle.

The results from above show no conclusive relationship between the nozzle diameter and the distance that the water travels. However, the graph does show that in general, decreasing the nozzle diameter does increase the distance the water travels. This is as expected, as decreasing the diameter increases the pressure of the water and therefore the velocity. A higher initial velocity leads to a longer distance travelled.

In addition, the graph also shows two results not following this relationship. Firstly, the nozzle diameter of 40mm only shows a small decrease in distance travelled when compared to a nozzle of 35mm. This could have been due to water starting to reach a limit, where the diameter of the nozzle is equal to the pipe diameter. This is as expected as the pumps exit diameter is 42mm, the same as the pipes.

Secondly, the nozzle diameter of 10mm doesn't increase the distance at which the water travelled and instead decreases the distance. This could have been down to many reasons, but the most probable is due to restrictions in water flow. Due to the diameter being so small, the water flow rate is restricted which means less water is being released but at an increased pressure. No conclusions can be drawn from this experiment but it could be used to try and find the optimum nozzle for distance.

5.1.1.2 Water Flow Rate

This experiment was done to find the flow rate of the water; the time was measured to see how long it would take to fill 3 gallons/13.64 litres. The same design used for the water range experiment was also used for this.

Flow Rate (L/s)	Nozzle Diameter (mm)
0.23	10
0.92	17
1.24	20
1.44	25
1.65	35
1.95	40

Table 5.2 shows results for the change in flow rate with a changing nozzle diameter

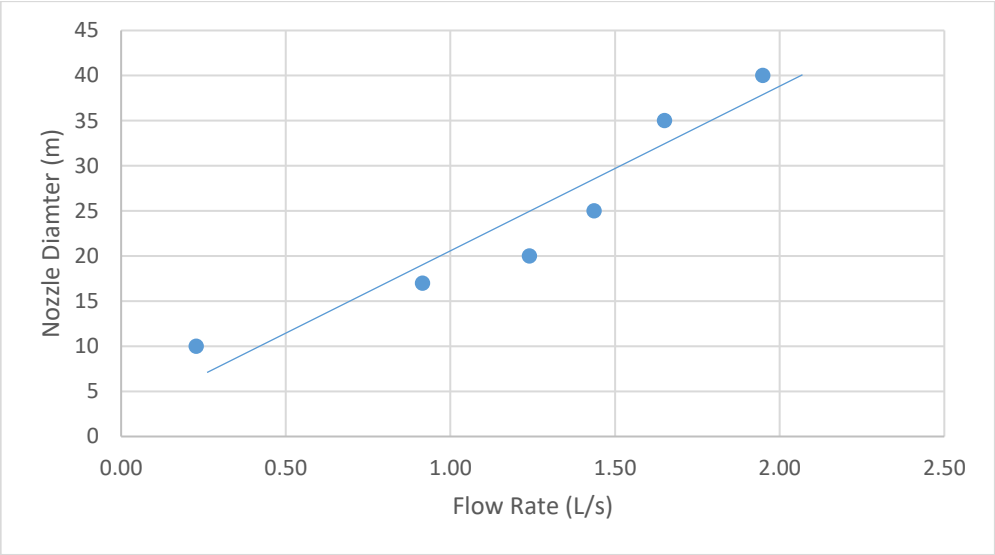

Figure 5.2 A graph showing the relationship between the flow rate (L/s) and the nozzle diameter

The results from this experiment, shown above in Figure 5.2, show that increasing the nozzle diameter increases the flow rate. This is as expected, as a smaller pipe has a smaller volume which means less water can flow through. The optimum flow rate seems to be the one closest to the diameter of the pumps exit of 40mm. However, from experiment 1 it was found that a nozzle of 40mm doesn't travel very far. This means that a balance must be found between distance travelled and the flow rate, as they seem to have an opposing relationship. More data needs to be found before a conclusive decision on nozzle diameter can be made.

From the results above it was clear that a nozzle diameter between 17 and 25mm produced the best for distance and flow rate. The next experiment was done to see how adding more exit points effected the distance travelled and the flow rate.

2 Nozzles

Nozzle Diameter (mm)	Flow Rate (L/s)	Distance Travelled (m)
17	1.45	2.8
20	1.84	1.7
25	2.35	1.20

Table 5.3 shows the results for the distance travelled and flow rate for a changing nozzle diameter, with 2 nozzles used.

3 Nozzles

Nozzle Diameter (mm)	Flow Rate (L/s)	Distance Travelled (m)
17	1.48	2.60
20	2.24	1.60
25	2.84	1.10

Table 5.4 shows the results for the distance travelled and flow rate for a changing nozzle diameter, with 3 nozzles used

The results from the table above show that two nozzles show an increase in flow rate when compared to one nozzle. This shows that adding another exit point for the water means that more can be distributed. In addition, the results also show that the distance travelled decreases when another nozzle is added. However, this isn't a substantial difference when compared to just using one exit point which could be beneficial.

5.1.1.3 Tube Length

This experiment was done to see how flow rate and water range changes with a longer pipe.

Pipe Length (m)	Range (m)	Total Distance (m)	Flow Rate Litres/s
0.4	2.2	2.6	1.49
1	2.1	3.1	1.45
1.8	2.0	3.92	1.26

Table 5.5 shows the results for the water range from the exit point, the total distance including the length of pipe and flow rate for a changing pipe length, with 1 nozzle used

The results from the above table, Table 5.5 show the difference a different length of pipe would make. It shows that increasing the pipe doesn't affect the distance at which the water travels from the exit. A small decrease is shown which could be down to the increase in height the water has to travel from the pump, meaning pressure will be lost. A longer pipe also shows a decrease in flow rate which could be because of the same reason, a loss in pressure.

5.1.2 Experiment 2

The second experiment was done to see how spinning the device would have an impact on the distance at which water travels and flows. Suitable adjustments and improvements were made to the first design, used in experiment 1, to accommodate the spinning. For this experiment a nozzle of 17mm was used to maximise the distance. The design explained in section 4.1.2 was used.

Nozzle Diameter (m)	Distance Travelled (m)	Distance Travelled spinning (m)
17	3.2	4.2

Table 5.6 shows the difference in distance travelled when spinning is introduced

From this experiment, it was found that spinning the device did increase the distance at which the water travels from the exit point. The distance was increased from 3.2m to 4.2m when spinning was introduced. This is as expected as spinning the device accelerates the rate at which water leaves the pipe, which is explained in section 3.4.2.2. From this experiment, no other key results were found, the flow rate didn't change when the device was spun.

5.2 Discussion

The most difficult challenge that had to be overcome during the project was that of achieving the distance necessary to make the project worthwhile on a 1/8th scale. During the first tests that were performed on the device, initial distances were not promising, only achieving a radius in the region of 3m, close to what was required of the device. The second design that was tested managed to reach the 4m radius mark, but to further the aim a lot of research was done into how maximum distance could be realised, with the final theoretical design featuring a new pump with a much higher head than the one that was previously used. The reasons that such a pump is only a theatrical part of the design at this point is that it would need to provide a large throughput of water and have a large head, which simply does not exist in the current market. It may be possible to get a pump custom built that can achieve something similar to what is required, but this would cost a great deal of money and take a large amount of time that was just not viable in the scope of the project.

To further aid the theory and to gain a better understanding of the feasibility of the project, small-scale experiments were to be done in a freezer. These experiments were to simulate a yearlong cycle of weather conditions in the Arctic over a 48-hour period. This would have been done by creating an ice sheet in a container of water during the winter period

and then simulating the melting from the Sun using a halogen lamp. Windy conditions were to be created with a set of computer fans in the freezer. Further experiments were to involve pumping water from beneath the ice to on top, as is the concept of the full-scale design. The experiments were to show how the water pumped to on top of the ice affected the ice thickness over the summer and winter months' simulation. To control and monitor the experiments many different instruments were to be designed and made. The monitoring devices needed for the design were temperature, wind speed and ice thickness. The greatest challenge faced was the ice thickness measurement, this was mainly due to the requirement of a high resolution for the small-scale experiments. Another challenge with this was that to test each new design and concept for the ice measurement circuit required a test over a 20 hour period to produce enough ice. This meant that designing and making the ice thickness measurement circuit for the small-scale experiments took much longer than anticipated, which meant that these experiments were unable to be done in the time frame available alongside the other research and experiments.

Conclusion and Future Work

6.1 Conclusion

The project undertaken covered a wide area of research, design and testing to gain a better understanding for the feasibility of the concept outlined in the introduction. In researching designs for each part of the unit a variety of different ideas and approaches were looked at. Many concepts were looked at for ways to harvest energy from the environment, distribute water across the required area and other such instrumentation. Some of these ideas were then discarded due to them being impractical and others through experimentation.

In addition, the aims and objectives of the project were met. A 1/8th scale model was produced based on the research done and the model was under the power requirements outlined to make the project achievable. After testing and improving the design based on the results, the unit was able to achieve the water spread required. From these early stage experiments and the research done the project goal of producing units that can harvest energy from the environment around them, and use it to pump water on top of the ice to thicken the ice sheets, appears to be attainable. The documentation of other research into the instrumentation for the full-scale device and for the small-scale experiments will allow for future research to be done to see how the thickness of ice sheets are affected by the pumping of water to the surface.

6.2 Future Work

Although a great deal of work has been put into the project, there is still a substantial amount that needs to be done in the future to ensure that it is feasible. One area to cover is to conduct the small-scale experiments in the freezer as was outlined in the discussion. This would give a better understanding of the ice thickness cycle over the Arctic year and how pumping water to on top of the ice would affect this.

Also, most of the required sensors for the full scale unit and experiments have been made, tested and calibrated. However, there were other sensors that need to be made and tested such as the flow rate sensor and wind speed sensor. Once all the sensors are made they then need to be combined into one system that can monitor and record all of them.

If the small-scale experiments show that the design could be implemented in the Arctic, the next stage would be to actually test the design in conditions a lot closer to ones present in the Arctic, such as a frozen lake in Scotland. There may be differences in how the

design operates on a full-scale model to how it operates inside the freezer, so everything needs to be tested again to ensure that it would not cause any issues. This could quite easily be initially done using the 1/8th scale model that has already been produced, checking how the ice will form once it is distributed as there is a worry that it may just form a wall around the design and not spread out to cover more area.

Another area of the project that was investigated was the use of a laminar flow nozzle to increase the distance that the water travelled and to limit the loss of water whilst in the air. Laminar flow nozzles are fairly simple to make, but due to time constraints in the project it was not possible to get one produced that could fit onto the design. If such a nozzle was produced, it would also require a heating element to be placed inside it and all the other pipes. This could be done using a resistive element that increased in its temperature when a voltage is applied over it. A research proposal is also being produced as it would be beneficial to allow future work to be carried out at the university, whether it be for a PHD or other form of research.

References

[1] A. MacMillan, “Global Warming Facts, Definition, Causes and Effects | NRDC,” Natural Resources Defense Council, 11 03 2016. [Online]. Available: https://www.nrdc.org/stories/global-warming-101. [Accessed 23 04 17].

[2] National Snow and Ice Data Center, “Charctic Interactive Sea Ice Graph,” National Snow and Ice Data Center, 04 12 2017. [Online]. Available: http://nsidc.org/arcticseaicenews/charctic-interactive-sea-ice-graph/. [Accessed 04 12 2017].

[3] A. Hall, “The Role of Surface Albedo Feedback in Climate,” *Journal of Climate,* vol. 17, no. 7, pp. 1510-1568, 2004.

[4] C. Deser, J. Walsh and M. Timlin, “Arctic Sea Ice Variability in the Context of Recent Atmospheric Circulation Trends,” *J Clim,* vol. 13, no. 3, pp. 617-633, 2000.

[5] “National Snow & Ice Data Center,” 2017. [Online]. Available: https://nsidc.org/cryosphere/seaice/processes/albedo.html.

[6] M. Winton, “Amplified Arctic climate change: What does surface albedo feedback have to do with it?,” *Geophysical Research Letters* , vol. 33, no. L03071, 2006.

[7] Oxford Dictionary, “definition of global warming in English - Oxford Dictionaries,” Oxford Dictionary, [Online]. Available: https://en.oxforddictionaries.com/definition/global_warming. [Accessed 2017 04 07].

[8] S. Eldredge and B. Biek, “Glad You Asked: Ice Ages – What are they and what causes them,” The Utah Geological Survey, september 2010. [Online]. Available: http://geology.utah.gov/map-pub/survey-notes/glad-you-asked/ice-ages-what-are-they-and-what-causes-them/. [Accessed 2017 04 07].

[9] D. Harris, “MONITORING GLOBAL WARMING,” *Energy And Environment,* vol. 22, no. 7, pp. 929-937, 2011.

[10] “Energy Fundamentals, Physics of Wind Turbines,” Leipzig University, 5 2015. [Online]. Available: http://home.uni-leipzig.de/energy/ef/15.htm.

[11] A. M. Ragheb, “Wind Turbines Theory - The Betz Equation and Optimal Rotor Tip Speed Rato, Fundamental and Advanced Topics in Wind Power,” InTech, 2011. [Online]. Available: http://www.intechopen.com/books/fundamental-and-advanced-topics-in-wind-power/wind-turbines-theory-the-betz-equation-and-optimal-rotor-tip-speed-ratio.

[12] Alphabet Energy, Inc., “How Thermoelectric Generators Work,” Alphabet Energy, Inc., [Online]. Available: https://www.alphabetenergy.com/how-thermoelectrics-work/. [Accessed 23 04 2017].

[13] M. Leppäranta and K. Myrberg, Physical Oceanography of the Baltic Sea, Chichester: Praxis Publishing, 2009.

[14] Meteoblue, “Weather history download Isachsen - meteoblue,” Meteoblue, [Online]. Available: https://www.meteoblue.com/en/weather/archive/export/isachsen_canada_5984185 . [Accessed 2017 04 15].

[15] Y. Y. a. G. A. M. D.A. Rothrock, “Thinning of the Arctic Sea-Ice Cover,” *GEOPHYSICAL RESEARCH LETTERS,* vol. 26, no. 23, pp. 3469-3472, 1999.

[16] T. S. Light, S. Licht, B. Anthony C and K. R. Morashc, “The Fundamental Conductivity and Resistivity of Water,” The Electrochemical Society, Massachusetts, 2005.

[17] M. Chaplin, “Water structure and science,” 2006. [Online]. Available: http://www1.lsbu.ac.uk/water/material_anomalies.html. [Accessed 5 January 2017].

[18] “Water Quality Monitoring: Conductivity,” Friends of Five Creeks, [Online]. Available: http://www.fivecreeks.org/monitor/cond.shtml.

[19] G. Falkovich, “Fluid Mechanics,” Cambridge University Press, 2011.

[20] G. B. J. H. T. L. H. J. Yan, “Model of droplet dynamics and evaporation for sprinkler irrigation,” *Biosystems Engineering,* vol. 106, no. 4, pp. 440-447, 2010.

[21] “The Onset of Turbulence in Pipe Flow,” *Science,* vol. 333, no. 6039, pp. 192-196, 2011.

[22] Learn Engineering, “Working of Centrifugal Pumps ~ Learn Engineering,” Learn Engineering, 01 01 2014. [Online]. Available: http://www.learnengineering.org/2014/01/centrifugal-hydraulic-pumps.html. [Accessed 24 04 2017].

[23] Frozee, “Centrifugal Pumps,” Marine Engineering Online, 30 04 2014. [Online]. Available: http://marineengineeringonline.com/centrifugal-pumps/. [Accessed 24 04 2017].

[24] Process Industry Forum, “What is a Positive Displacement Pump,” Process Industry Forum, 26 08 2013. [Online]. Available: http://www.processindustryforum.com/article/different-types-pumps-positive-displacement-pumps. [Accessed 25 04 17].

[25] hyperphysics, “How does an electric motor work?,” hyperphysics, [Online]. Available: http://hyperphysics.phy-astr.gsu.edu/hbase/magnetic/mothow.html.

[26] Makivik Corporation, “Nunavik Maps - Makivik Corporation,” Makivik Corporation, [Online]. Available: http://www.makivik.org/wp-content/uploads/2013/02/canadian_inuit_map.gif. [Accessed 14 04 2017].

[27] DEPARTMENT OF EXECUTIVE AND INTERGOVERNMENTAL AFFAIRS, “Population Data | Government of Nunavut,” 01 07 2016. [Online]. Available: http://www.gov.nu.ca/eia/information/population-data. [Accessed 14 04 2017].

[28] D. Wilson and D. Macdonald, THE INCOME GAP BETWEEN ABORIGINAL PEOPLES AND THE REST OF CANADA, Ottawa: Canadian Centre for Policy Alternatives, 2010.

[29] S. J. Desch et al., “Arctic Ice Management,” *Earth’s Future,* vol. 5, no. 1, pp. 107-127, 2017.

[30] M. S. H. Eicken, Field Techniques For Sea Ice Research, University of Alaska Press, 2010.

[31] J. Q. X. D. L. Cui, “Freshwater ice thickness apparatus based on differences in electrical resistance and temperature,” *Cold Regions Science and Technology*, vol. 119, pp. 37-46, 2015.

[32] U. o. California, “Lecture 4: Circuilation and Vorticity,” University of California, [Online]. Available: https://www.ess.uci.edu/~yu/class/ess227/lecture.4.vorticity.all.pdf.

[33] V. Bladeless, “Homepage,” Vortex Bladeless, [Online]. Available: http://www.vortexbladeless.com/.

[34] V. Bladeless, “Vortex Crowdfunding Campaign on Indiegogo.,” Vortex Bladeless, [Online]. Available: https://youtu.be/WqcNc9bKlNY?t=47s.

[35] L. STINSON, “The Future of Wind Turbines? No Blades,” Wired, [Online]. Available: https://www.wired.com/2015/05/future-wind-turbines-no-blades/.

[36] KITEnrg, “High-altitude wind technology | kite energy | power kite,” KITEnrg, [Online]. Available: http://www.kitenergy.net/technology-2/key-points/. [Accessed 24 04 2017].

[37] rule, “Standard Bilge Pump - Technical Data Sheet - Multilingual,” 1 10 2012. [Online]. Available: http://www.xylemflowcontrol.com/files/950-0518.pdf. [Accessed 25 04 2017].

[38] Calibrate, “Anemometer and Wind Speed Calibration Services,” [Online]. Available: http://www.calibrate.co.uk/anemometers/.

[39] B. Benchoff, “ULTRASONIC ANEMOMETER FOR AN ABSURDLY ACCURATE WEATHER STATION,” HACKADAY, 21 09 2013. [Online]. Available: http://hackaday.com/2013/08/21/ultrasonic-anemometer-for-an-absurdly-accurate-weather-station/. [Accessed 27 04 17].

[40] “HRXL-MaxSonar®-WRS3,” [Online]. Available: http://www.maxbotix.com/Ultrasonic_Sensors/MB7334.htm. [Accessed 1 April 2017].

[41] S. M. Pershin, V. N. Lednev, V. K. Klinkov, R. N. Yulmetov and A. F. Bunkin, “Ice thickness measurements by Raman scattering,” 2014.

[42] “Beaufort Gyre Exploration Project,” Woods Hole Oceanographic Institution, 18 October 2016. [Online]. Available: http://www.whoi.edu/page.do?pid=147516&tid=201&cid=116773&ct=8822&print=this. [Accessed 18 March 2017].

[43] Universal Flow Monitors, Inc. , “Ultrasonic Flowmeter Technology - Flowmeters.com,” Universal Flow Monitors, Inc. , [Online]. Available: http://www.flowmeters.com/ultrasonic-technology. [Accessed 27 04 2017].

[44] Sparkfun, “SparkFun Hall-Effect Current Sensor Breakout - ACS712,” Sparkfun, 2017. [Online]. Available: https://www.sparkfun.com/products/8882.

[45] k. systems, “30A SCT-013-030 Non-invasive AC current sensor Split Core Current Transformer AL,” ktechnics systems, [Online]. Available: http://ktechnics.com/shop/30a-sct-013-030-non-invasive-ac-current-sensor-split-core-current-transformer-al/.

[46] Wikipedia, “Raspberry Pi,” Wikipedia, 2017. [Online]. Available: https://en.wikipedia.org/wiki/Raspberry_Pi#Specifications.

[47] C. Stanton, “A Comprehensive Raspberry Pi 3 Benchmark,” Element 14, [Online]. Available: https://www.element14.com/community/community/raspberry-pi/blog/2016/02/29/the-most-comprehensive-raspberry-pi-comparison-benchmark-ever.

[48] G. Factory, “Implementing SPI & I2C Interfaces On Papilio One,” Gadget Factory, 2017. [Online]. Available: http://blog.gadgetfactory.net/2013/04/implementing-spi-i2c-interfaces-on-papilio-one/.

[49] G. C. Diyoke, O. C. and U. Aniagwu, “Different Methods of Speed Control of Three-Phase Asynchronous Motor,” *American Journal of Electrical and Electronic Engineering,* vol. 4, no. 2, pp. 62-68, 2016.

[50] Wikipedia, “Wireless Ad Hoc Network,” Wikipedia, [Online]. Available: https://en.wikipedia.org/wiki/Wireless_ad_hoc_network.

[51] Oasis, “MQTT Version 3.1.1 Plus Errata 01,” Oasis, 10 December 2015. [Online]. Available: http://docs.oasis-open.org/mqtt/mqtt/v3.1.1/errata01/os/mqtt-v3.1.1-errata01-os-complete.html#_Toc442180821.

[52] Rule, “Model 56D, 56D-24, 56D-32,” 2004. [Online]. Available: http://www.safety-marine.co.uk/downloads/Rule-4000gph-Bilge-Pump-Instruction-Sheet.pdf?did=297. [Accessed 23 04 2017].

[53] S. Jayanti, “Bends, Flow and Pressure Drop in,” Thermopedia, February 2011. [Online]. Available: http://www.thermopedia.com/content/577/.

[54] “KB817 Datasheet,” Knightbright, 26 April 2012. [Online]. Available: http://www.kingbrightusa.com/images/catalog/SPEC/KB817-B.pdf.

[55] Analog Devices, 2016. [Online]. Available: http://www.analog.com/media/en/technical-documentation/data-sheets/AD623.pdf.

[56] Wikipedia, “Thermoelectric Effect,” Wikipedia, [Online]. Available: https://en.wikipedia.org/wiki/Thermoelectric_effect.

[57] thermoelectrics, “Thermoelectric power generation - thermoelectric power generator,” [Online]. Available: https://i.ytimg.com/vi/YhynSkFlJOs/maxresdefault.jpg.